

NATIONAL AERONAUTICS AND SPACE ADMINISTRATION

CASE FILE
Technical Report 32-1315 **COPY**

*Electromagnetic Interference Aspects
of Integrating a UHF/VHF Receiver
Onboard Mariner V*

Richard K. Case

Louis H. Keeler

**JET PROPULSION LABORATORY
CALIFORNIA INSTITUTE OF TECHNOLOGY
PASADENA, CALIFORNIA**

November 1, 1968

NATIONAL AERONAUTICS AND SPACE ADMINISTRATION

Technical Report 32-1315

*Electromagnetic Interference Aspects
of Integrating a UHF/VHF Receiver
Onboard Mariner V*

Richard K. Case

Louis H. Keeler

JET PROPULSION LABORATORY
CALIFORNIA INSTITUTE OF TECHNOLOGY
PASADENA, CALIFORNIA

November 1, 1968

TECHNICAL REPORT 32-1315

Copyright © 1968
Jet Propulsion Laboratory
California Institute of Technology

Prepared Under Contract No. NAS 7-100
National Aeronautics & Space Administration

Preface

The work described in this report was performed by the Project Engineering Division of the Jet Propulsion Laboratory.

Acknowledgment

The authors wish to acknowledge the efforts of the personnel associated with the *Mariner Venus 67* project who contributed to the successful integration of the DFR onboard *Mariner V*. Special thanks go to members of the *Mariner V* test team who ungrudgingly conducted tests from 10 p.m. to 6 a.m. Special thanks also go to Tay Howard, DFR Project Manager, Stanford University, and Roy Long, DFR Project Engineer, Stanford Research Institute, who actively participated in the integration effort.

Contents

I. Introduction	1
II. Spacecraft and Dual Frequency Receiver	2
A. Mission Description and Objective	2
B. DFR Experiment	2
C. Spacecraft Description	2
D. DFR Operational Description	4
III. Initiation of Electromagnetic Compatibility Program	6
A. Preliminary Analysis	6
B. Test Philosophy	6
C. Test Instrumentation	8
1. UHF noise detection instrumentation	8
2. VHF noise detection instrumentation	9
3. Portable VHF/UHF low-noise receiver	9
D. Noise Level Calculations	12
IV. Evaluation of <i>Mariner V</i> UHF/VHF Noise Environment	13
A. DFR/S-Band Transponder Test	13
1. Interaction of local oscillator harmonics	15
2. Intermodulation interference	15
3. Interaction between S-band transmitter outputs and the DFR	15
4. Interaction between DFR outputs and the S-band receiver	15
B. System Level Tests	17
1. Power subsystem noise investigation — booster regulators	18
2. Battery charger	20
C. S-Band Transmitter Power Supply Noise Investigation	20
D. DAS Noise Investigation	20
E. Spacecraft Noise Level Verification Test	22
F. Summary of Results	26
V. Conclusions	26
Appendix. Example Noise Level Calculation	28

Contents (contd)

References	29
Bibliography	29

Table

1. Electromagnetic interference summary	27
---	-----------

Figures

1. Occultation trajectory	2
2. Spacecraft configuration (earth side)	3
3. Spacecraft configuration (sun side)	3
4. DFR block diagram	5
5. DFR	6
6. Noise coupling	7
7. Low-noise preamplifiers	9
8. Noise detection instrumentation console	10
9. UHF noise detection instrumentation block diagram	11
10. VHF noise detection instrumentation block diagram	12
11. DFR/S-band transponder test configuration	14
12. DFR/S-band antenna coupling measurements	16
13. DFR antennas and filters	17
14. Spacecraft test configuration	18
15. Power subsystem noise sources	19
16. DAS master oscillator harmonics	21
17. Spacecraft science case	22
18. Suspended spacecraft	23
19. Spacecraft instrumentation configuration for noise measurements	24
20. Noise level changes vs antenna noise temperature	25
21. Dual frequency receiver test configuration	26

Abstract

On a spacecraft, electronic equipment in close proximity must operate in the environment of noise generated by every other device on that spacecraft. When the electronic equipment is a sensitive radio receiver, the spacecraft noise can affect the sensitivity of the receiver if the noise is in its passband. The tasks involved in the integration of a dual frequency receiver (DFR) on *Mariner V* as part of the complement of scientific instruments are discussed in this report. The primary effort was that of ensuring proper experiment operation after it was determined that noise contributed by the spacecraft was excessive at 49.8 MHz and that there was an interaction of the DFR 423.3-MHz channel with the S-band telecommunications ranging system. The criteria for verifying proper system operation and the modifications necessary for establishing a compatible spacecraft environment are discussed.

Electromagnetic Interference Aspects of Integrating a UHF/VHF Receiver Onboard *Mariner V*

I. Introduction

Because interference is a distinct possibility for radio subsystems in close proximity to electronic devices, and because radio receivers can be seriously degraded by radio frequency noise, formal electromagnetic interference (EMI) assessments of the *Mariner V* spacecraft and the UHF/VHF receiver (DFR) experiment were initiated. Initial concern was that the spacecraft S-band communications subsystem and the DFR experiment contained signals that would directly interfere with one another. Also of concern was that RF noise generated by the spacecraft would degrade DFR performance, thereby jeopardizing the experiment.

The primary objective of the DFR experiment was to measure the dispersive doppler of radio signals that have traveled from an earth-based transmitter to the *Mariner V* spacecraft. Measurements of dispersive doppler are used to calculate the electron density of the column of space between the transmitter and the receiver. As the spacecraft passed Venus, the radio waves had to travel through the planet's ionosphere and atmo-

sphere to be received by the DFR, thus enabling measurements of the electron density of the planet's ionosphere and atmosphere. Electromagnetic energy traveling through a dense atmosphere, such as predicted for Venus, is de-focused, scattered, and absorbed, resulting in large decreases in signal strength at the receiver. Obviously, for radio waves to be received through a dense atmosphere requires high-powered transmitters and sensitive receivers.

The effective sensitivity of a receiver is a function of the background noise level in which it must operate. For receivers such as the DFR, with signal thresholds of -140 dBmW, extremely low-level noise in the receivers' passband can degrade their performance. Background noise for an interplanetary mission can be grouped into two classes: cosmic and spacecraft. For any given system, there is no control over the level of cosmic noise that exists in the receiver's passband, but the level of noise generated by the spacecraft can be controlled. The principal purpose of this report is to discuss the efforts to reduce spacecraft-generated noise.

II. Spacecraft and Dual Frequency Receiver

A. Mission Description and Objective

Mariner V was launched on June 14, 1967 from Cape Kennedy, Florida by an *Atlas D/Agna D* launch system. The spacecraft flight path took it to within 2460 mi of Venus on October 19, 1967 after 127 days of flight.

The primary objective of the *Mariner Venus 67* project was to conduct a flyby mission to Venus to obtain scientific information that would supplement and extend the results obtained in 1962 by *Mariner II* relevant to the origin and nature of Venus and its environment.

The secondary objectives were to acquire engineering experience in converting and operating a spacecraft designed for flight to Mars into one flown to Venus, and to obtain information on the interplanetary environment during a period of increasing solar activity.

B. DFR Experiment

The DFR had previously been used on two *Pioneer* spacecraft to measure the electron density of interplanetary space. For the *Mariner V* mission, the experimental objectives were extended to include measurements of the atmospheric and ionospheric characteristics of Venus. Investigation of planetary atmospheres, using electromagnetic radiation, is accomplished by launching spacecraft on trajectories that will enable earth-based transmitters to transmit radio waves through the planet's atmosphere and ionosphere to receivers onboard the spacecraft. Trajectories that require earth-based signals to travel through a planet's atmosphere prior to reaching the spacecraft result in the planet occulting the spacecraft as viewed from earth. An earth occultation trajectory is shown in Fig. 1.

Because the electromagnetic radiation travels through the planet's atmosphere before it reaches the receiver, certain changes occur in the wavelength, phase, and amplitude of the signal, which would not have occurred if the signal were to have travelled through free space. The changes in the signal received at the spacecraft occur because the index of refraction of the planetary atmosphere and ionosphere differs from the unity index of refraction for free space. Therefore, the phase velocity of propagation is changed according to the relationship between the velocity of propagation in free space, c , the phase velocity of propagation in the medium, v_p , and the index of refractivity μ ; $v_p = c/\mu$. For an ionized medium, μ is less than 1 and the phase velocity of the wave

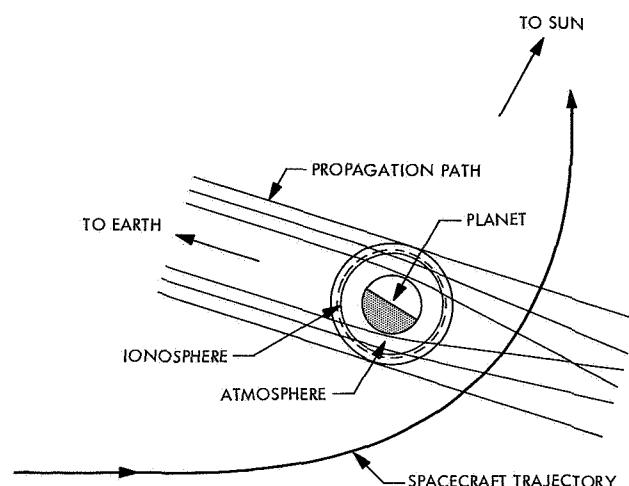


Fig. 1. Occultation trajectory

increases. For a neutral atmosphere, the index of refraction is greater than 1 and the phase velocity is decreased. These changes in the velocity of propagation of the electromagnetic radiation, as it travels through the planet's atmosphere and ionosphere, make the radio waves appear to have travelled a distance different from that expected from the spacecraft trajectory. Also, any nonuniformity of the medium through which the wave travels results in a nonuniform index of refraction. This nonuniformity causes various points on the radio wave fronts to travel at different speeds. As a result, the path of the radio wave deviates from a straight line, causing an increase in the path length and a focusing and defocusing of the radio waves. The changes in path length appear at the receiver as a frequency shift, while the focusing effects result in a change in signal strength. By measuring the time rate of change of frequency and amplitude, a value for the time rate of change of index of refraction can be obtained. The values of the index of refraction can then be used with parameters available from earth-based measurements to develop a model of the planet's atmosphere.

C. Spacecraft Description

The *Mariner V* shown in Figs. 2 and 3 was an extension of the *Mariner C* design — an octagon that provided eight bays for housing electronic equipment and a trajectory correction rocket motor. The spacecraft weighed 540 lb and was three-axis stabilized using the sun and the star Canopus as references. Power was provided by a battery and photovoltaic cells arranged on four fixed-position solar panels. The battery provided power during the launch-to-solar acquisition phase, during maneuvers, and whenever spacecraft power demands exceeded the

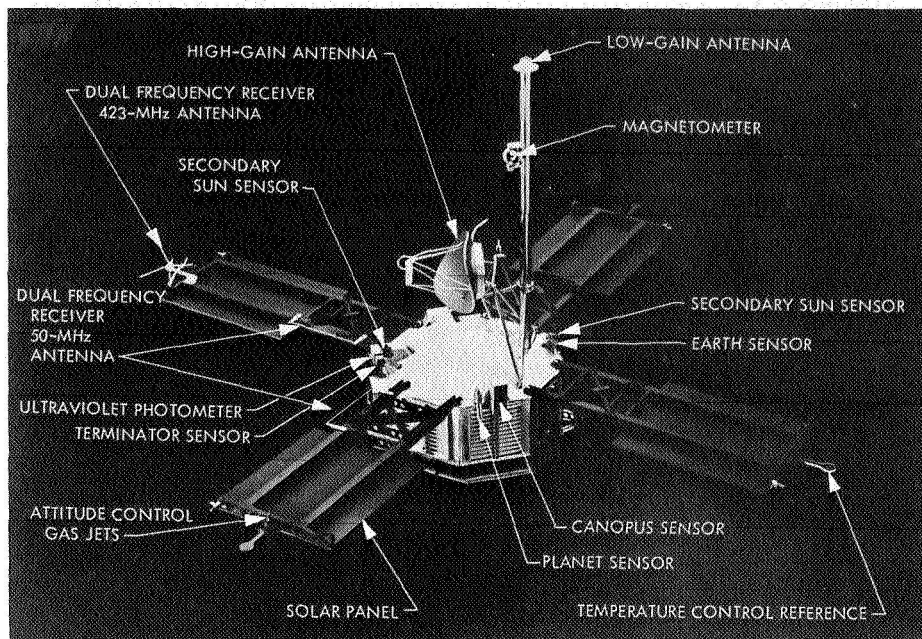


Fig. 2. Spacecraft configuration (earth side)

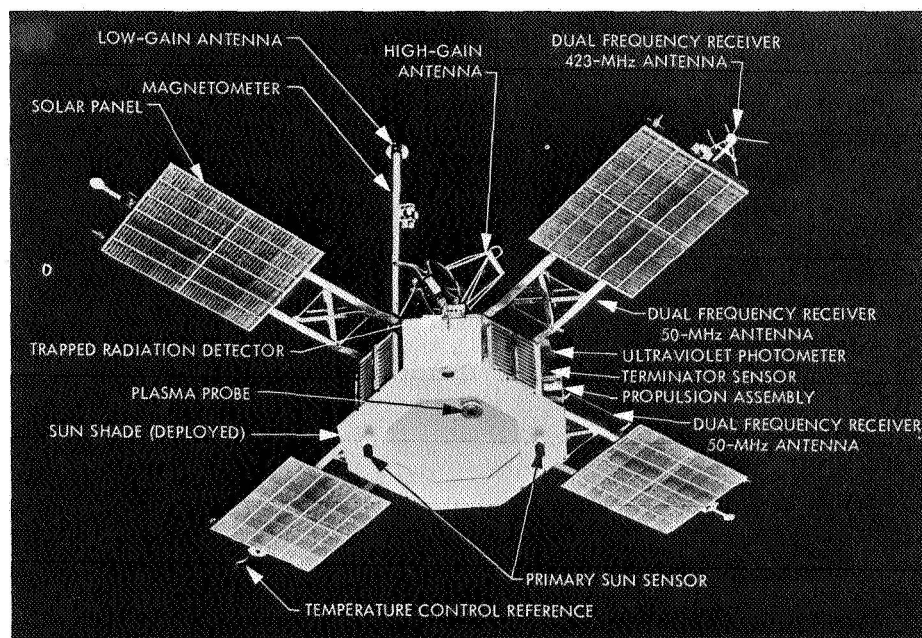


Fig. 3. Spacecraft configuration (sun side)

solar panel capabilities. The spacecraft had an S-band communications system which provided telemetry information to earth, command capability to the spacecraft, and tracking information for orbit determination. The spacecraft was fully automatic and, once injected on the proper trajectory, onboard equipment could successfully complete the mission. However, radio command capability existed as a backup to certain mandatory spacecraft operations as well as to provide switching capability of onboard spacecraft logic and redundant equipment. The spacecraft command subsystem consisted of 29 discrete commands and 1 quantitative command. The quantitative command was coded into three separate commands for use by the central computer and sequencer for timing the trajectory correction maneuver pitch, roll, and motor burn durations.

The spacecraft carried five scientific instruments for investigating interplanetary space during the flight and near Venus: (1) a trapped radiation detector, (2) a plasma probe, (3) a magnetometer, (4) an ultraviolet photometer, and (5) the DFR. The S-band transponder also served as a scientific instrument since it was used as part of an S-band occultation experiment.

D. DFR Operational Description

The DFR was a two-channel, UHF/VHF, phase-locked, double-conversion superheterodyne receiver. The receiver consisted of two phase-locked loops, operating at received frequencies of 49.8 and 423.3 MHz, plus the circuitry required to prepare data for transmission by the spacecraft telemetry subsystem. The receiver operated at a fixed gain of approximately 30 dB greater than required to limit on noise alone.

Harmonically related, coherent, continuous wave signals were transmitted to the receiver from a 150-ft parabolic antenna located near Stanford University, Stanford, Calif. Transmitter power during the encounter phase of the mission was 350 and 30 kW for the 49.8- and 423.3-MHz channels, respectively. The RF carriers could be phase-modulated with either an 8.692- or a 7.692-kHz signal for determining changes in group velocity.

The 49.8-MHz signal was received at the spacecraft by a fixed, linearly polarized antenna consisting of two adjacent shunt-fed solar panels. The gain of this antenna in the direction of earth at encounter was approximately 0 dB. The 423.3-MHz antenna was a quarter wave-length stub with four elements spaced 90 deg apart to form a

ground plane. Two of the four ground plane elements had reflectors mounted on them so that a gain of approximately 6 dB would be obtained in the direction of earth at encounter. The 423.3-MHz antenna was mounted on the end of a solar panel. The antennas are shown mounted on the spacecraft in Figs. 2 and 3.

A block diagram of the DFR is given in Fig. 4. Both channels of the receiver were identical, except for the RF amplifiers and first mixer stages, and are phase-locked by separate voltage-controlled crystal oscillators. First mixer injection for both channels was derived from the voltage control oscillator (VCO) in the 423.3-MHz channel. By using the output of the 423.3-MHz channel VCO to generate the first intermediate frequency for both channels, the 49.8-MHz channel and the 423.3-MHz channel are coherent.

By counting the positive and negative zero crossings of the frequency difference between VCO-1 and VCO-2, the frequency shift of the received signals was determined. The number of zero crossings was accumulated by a ten-bit counter that was nondestructively read out upon command from the spacecraft science data automation subsystem. These data were transmitted to earth for use in calculating certain characteristics of the medium through which the wave had traveled, such as electron density and refractivity. Differential group path measurements were also made by comparing the phase of the phase modulation on the two received signals. To evaluate receiver performance and to detect large frequency changes, both VCO control voltages (loop stress) were monitored. The output of the amplitude phase detectors in each channel was also monitored so that receiver signal-to-noise ratios could be determined.

The receiver was calibrated every 7 hours by connecting the output of the first mixer of the 423.3-MHz channel to the input of the first intermediate frequency (IF) of the 49.8-MHz channel, while removing the 49.8-MHz signal. In this operational mode, any output of the Δf or the modulation phase detectors other than zero represented an error source in the instrument. Any errors measured during the calibration cycle were used to correct the data.

The receiver (Fig. 5) had a 49.8-MHz channel noise temperature of 300°K and a 423.3-MHz channel noise temperature of 1200°K. It required approximately 1.8 W of power from a 2.4-kHz 100-V peak-to-peak power source and was contained in a 6¼- × 6- × 6-in. module. The receiver weighed 5.1 lb.

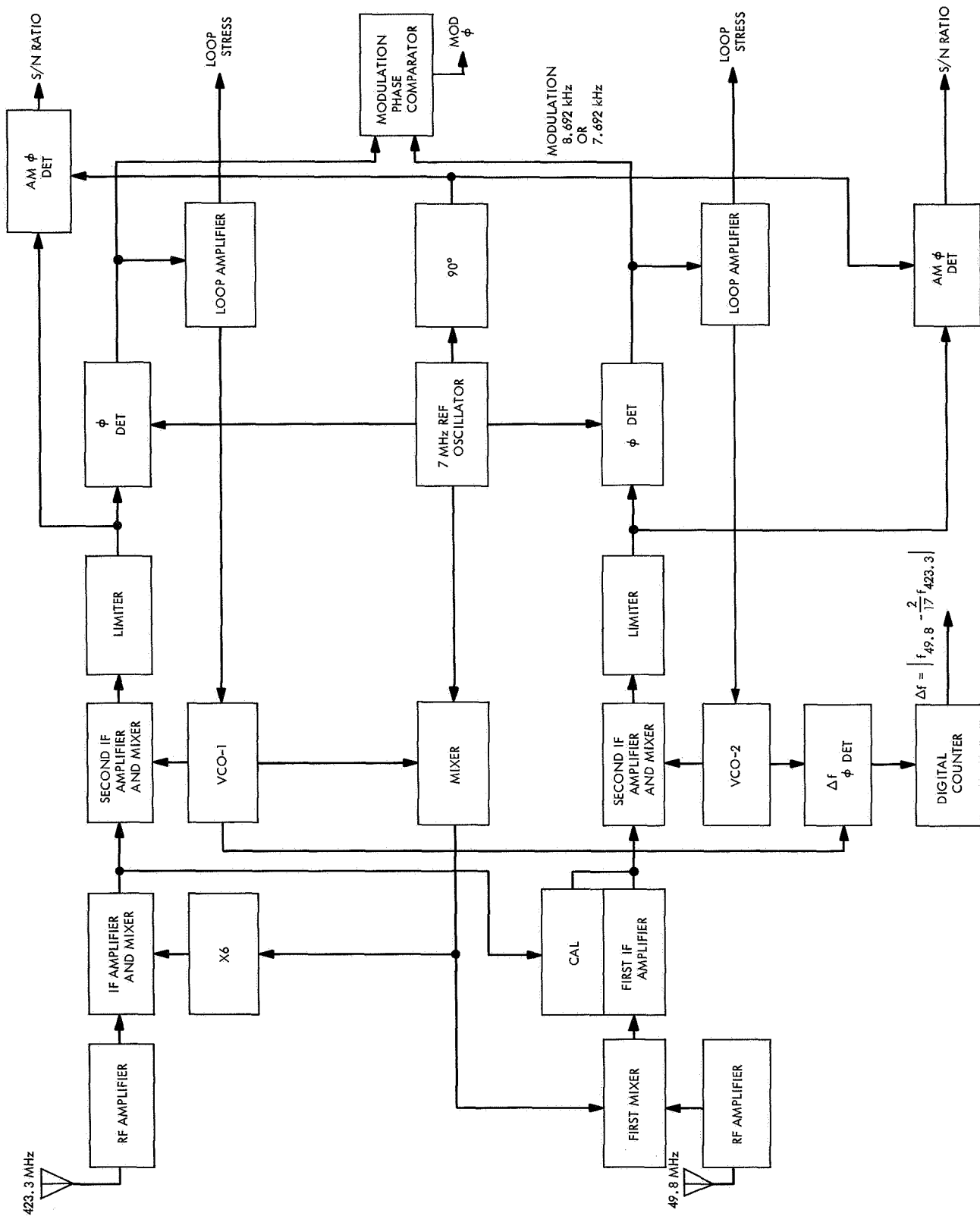


Fig. 4. DFR block diagram

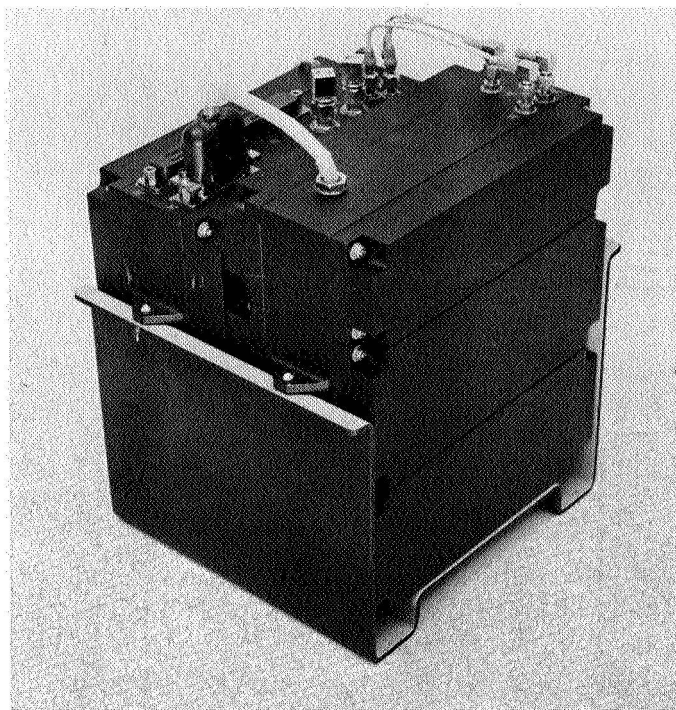


Fig. 5. DFR

III. Initiation of Electromagnetic Compatibility Program

A. Preliminary Analysis

The DFR integration effort began by reviewing data obtained about the DFR from the *Pioneer* space program, which had flown two DFRs. Personnel at the cognizant NASA center were interviewed to determine problem areas. The results of subsystem level electromagnetic interference tests performed on the DFR per Specification MIL-I-26600 (USAF) were obtained and reviewed. Examination of the EMI data showed that possible interfering signals of 9 and 19 MHz were radiated by the DFR and that the DFR was susceptible to frequencies from 50 to 200 Hz injected onto its +28-V dc power line.

A computer program was written as part of the analysis effort to determine possible intermodulation products that could exist on the spacecraft, and which would cause interference to the DFR or the S-band transponder. Two potentially disruptive frequencies were determined. These frequencies are listed in Section IV-A-2.

Three principal areas of concern regarding the ability of the DFR experiment to perform satisfactorily on *Mariner V* resulted from the initial study. First, although the DFR was a phase-locked receiver, it was sensitive to

low-level RF energy in its frequency band. The second area of concern was the power levels of the fundamental and harmonics of the 30- and 350-kW DFR ground transmitter frequencies. The fifth harmonic of 423.3 MHz is 2116.5 MHz, while the *Mariner V* S-band receiver frequency was 2115.7 MHz, with a 7-MHz intermediate frequency amplifier bandwidth. With the 423.3-MHz ground transmitter operating at its 30-kW output level, there was the possibility that the fifth harmonic would be of sufficient magnitude for the S-band receiver to acquire phase-lock, particularly during the near-earth portion of the mission. In addition, it was possible that the 49.8-MHz ground transmitter operating at its 350-kW output might interfere with the 47.8-MHz intermediate frequency of the S-band receiver. However, calculation of the expected RF power density levels indicated that, in the event of maximum DFR ground transmitter power emission during the first view of the spacecraft, no interference would be expected. It was also estimated that the fifth harmonic of the 423.3-MHz transmitter would be sufficiently suppressed. To ensure that ground transmitter harmonics would not be a problem, it was recommended that measurements be performed on the harmonics of concern to verify that the radiated levels would not affect the spacecraft transponder. As a safety factor, a restriction was placed on ground transmitter power output such that the received power level at the DFR was never to exceed -100 dBmW.

Finally, reports of DFR performance degradation on the *Pioneer* spacecraft caused apprehension for the successful operation of the instrument on *Mariner V*. A discrepancy of 17 dB between calculated and observed signal strength was observed on the 49.8-MHz channel, and a 2- to 5-dB discrepancy was observed on the 423.3-MHz channel. The observed discrepancies could be explained by excessive noise coupling into the receiver. The magnitude of the noise necessary to cause a 17-dB reduction in signal-to-noise ratio strongly suggested that the spacecraft was the major source of noise.

During this investigation, it became necessary to establish levels of maximum permissible noise degradation to the DFR. The principal investigator for the experiment contributed to this effort by specifying that there should be no more than a 3-dB degradation to the 49.8-MHz channel, and no more than a 1-dB degradation to the 423.3-MHz channel.

B. Test Philosophy

During the *Mariner* program, all subsystems were subjected to environmental acceptance tests encompassing

shock, vibration, and temperature vacuum. Electromagnetic interference tests were not included. However, if these tests had been performed on each subsystem, the task of predicting interference in a completely integrated spacecraft would have been an extremely complex task. The effects of electromagnetic emission from a subsystem can be significantly different in a test configuration than in a system configuration. Not only are noise levels important, but so are coupling factors. High-level noise signals that are loosely coupled to susceptible devices may not be as serious as low-level noise signals that are tightly coupled. Therefore, to completely evaluate the system compatibility of two subsystems based on subsystem noise measurements, it is necessary to know the coupling coefficients between the noise source and the measuring device for the subsystem configuration, and the noise source and the susceptible device for the system configuration.

Figure 6 illustrates a system and subsystem configuration for evaluating radiated noise. The system noise level

at any location on the spacecraft resulting from any given subsystem could be calculated from subsystem noise measurements by multiplying the subsystem noise level by the coupling coefficients.

$$N_L = N_D \left(\frac{C_2(f, g)}{C_1(f, g)} \right) \quad (1)$$

where

N_L = system noise level at the susceptible device

N_D = subsystem noise level measured during subsystem test

$C_1(f, g)$ = subsystem level coupling coefficient between noise source and noise detector. A function of frequency and geometry.

$C_2(f, g)$ = system level coupling coefficient between noise source and susceptible device. A function of frequency and geometry.

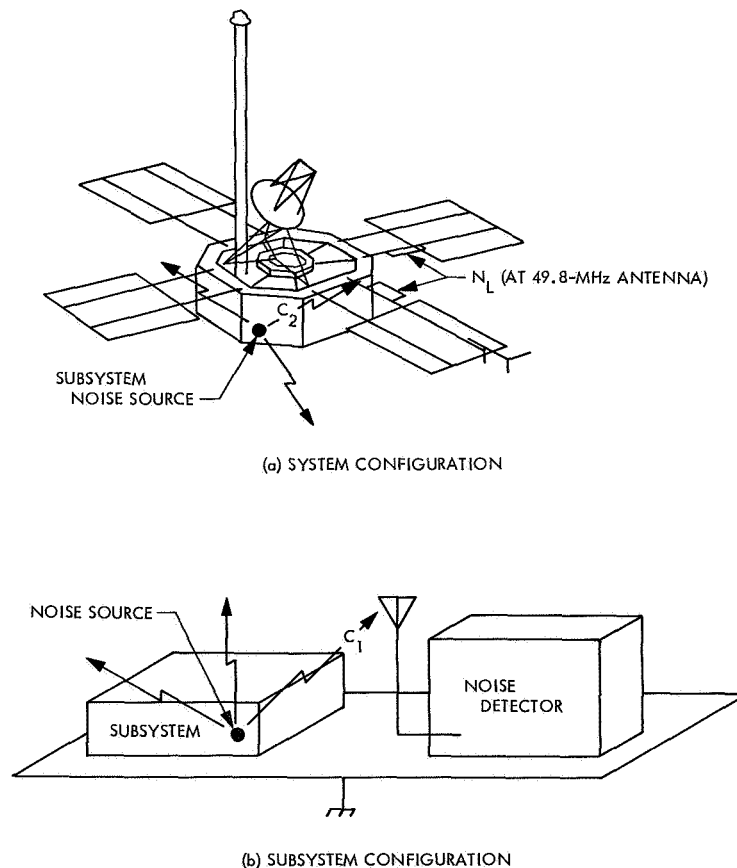


Fig. 6. Noise coupling

The difficulty in calculating system noise levels is in determining the coupling coefficients C_1 and C_2 . Because the system configuration presented a complex arrangement of circuit elements, circuit wiring, and interconnecting and intraconnecting cabling that acted as antennas, no practical method was available for calculating system level coupling coefficients. If coupling coefficients were to be determined, they would have to be determined experimentally during special coupling tests. To obtain any accuracy in system level coupling coefficients a major portion of the spacecraft electrical and mechanical assemblies would be required. Once the spacecraft was assembled into the configuration necessary to evaluate system level coupling coefficients, direct measurements of noise levels at the DFR antennas from subsystem noise sources were possible. It would, therefore, have been illogical to determine the system level coupling coefficients (C_2) between subsystem noise sources and the DFR antennas when it was possible to measure the noise levels directly. Without the values of C_2 , subsystem noise measurement would serve only as a cursory indication of possible interference; therefore, it was concluded that electromagnetic compatibility testing would have to be performed with all the subsystems assembled on the spacecraft.

There was one area in which coupling coefficients could be determined prior to assembling the spacecraft. It was possible to measure DFR antenna-to-S-band antenna coupling factors because a full-scale model of the spacecraft was built early in the program for use in developing the *Mariner V* antennas. Since the coupling factors between the DFR and the S-band transponder antennas could be measured, subsystem tests to determine the RF signature and the noise susceptibility of each subsystem at their antenna terminals would provide the data necessary to use Eq. (1) to evaluate this aspect of system compatibility.

Although quantitative subsystem noise tests were possible only with the S-band transponder, qualitative tests were performed on many subsystems using a small portable test receiver. A brief description of this receiver is given in Section III-C-3. Tests were performed with the portable test receiver to determine the relative levels of noise a subsystem might be generating at the frequencies to which the DFR was susceptible. This portable test receiver provided the ability to identify potential noise sources during cursory RF noise tests performed in the subsystem laboratories as soon as the subsystems were delivered from the manufacturer.

C. Test Instrumentation

The test instrumentation was required to scan a frequency range of ± 200 kHz, centered at the DFR frequencies, with a bandwidth of 1 kHz or less. The narrow bandwidth capability was required to provide resolution of the noise spectra as well as aid in identifying discrete frequencies during a frequency scan. Noise figures lower than the 3- and 7-dB values for the DFR were required to provide confidence in the test data. Low-noise figures were also required to prevent test instrumentation noise from masking spacecraft noise.

The design of the test instrumentation was based on commercially available low-noise RF preamplifiers and frequency converters and a military R390A/URR high-frequency receiver having narrow bandwidth mechanical filters and accurate frequency readout. The low-noise preamplifiers are shown in Fig. 7. The output of the preamplifiers was mixed with a local oscillator frequency to translate the signals received by the preamplifiers to the frequency range of the R390A/URR high-frequency receiver (0.5 to 32 MHz). The 455-kHz intermediate frequency of the R390A/URR, available at selectable bandwidths of 0.1, 1, 2, 4, 8, and 16 kHz, was used to monitor the signals received by the preamplifiers. The frequency and amplitude of the received RF energy was analyzed by monitoring the 455-kHz IF output of the R390A/URR with a true rms voltmeter and a panadapter (a Panoramic Electronics SB-12b spectrum analyzer operating at a center frequency of 455 kHz). The rms voltmeter (Ballantine model 320) measured the true rms value of complex wave forms with all significant components in the range of 5 to 500 kHz. The panadapter enabled examination of the noise spectra of the signal received by the R390A/URR. It was desirable that the local oscillators for the frequency converters be stable enough to maintain the center frequency within a bandwidth of 1000 Hz on the R390A/URR receiver during a measurement period of approximately 20 min. The local oscillator stability satisfied this requirement. A frequency counter was used to monitor the local oscillator frequency so as to provide the capability for determining the frequency of discrete RF signals to the accuracy of the R390A/URR receiver. The noise detection instrumentation console is shown in Fig. 8.

1. UHF noise detection instrumentation. The instrumentation block diagram for analyzing UHF noise at 423.3 and 473.1 MHz is shown in Fig. 9. The preamplifier/mixer was a commercially available low-noise module with a gain of 30 dB and a noise figure of 2.0 dB. By

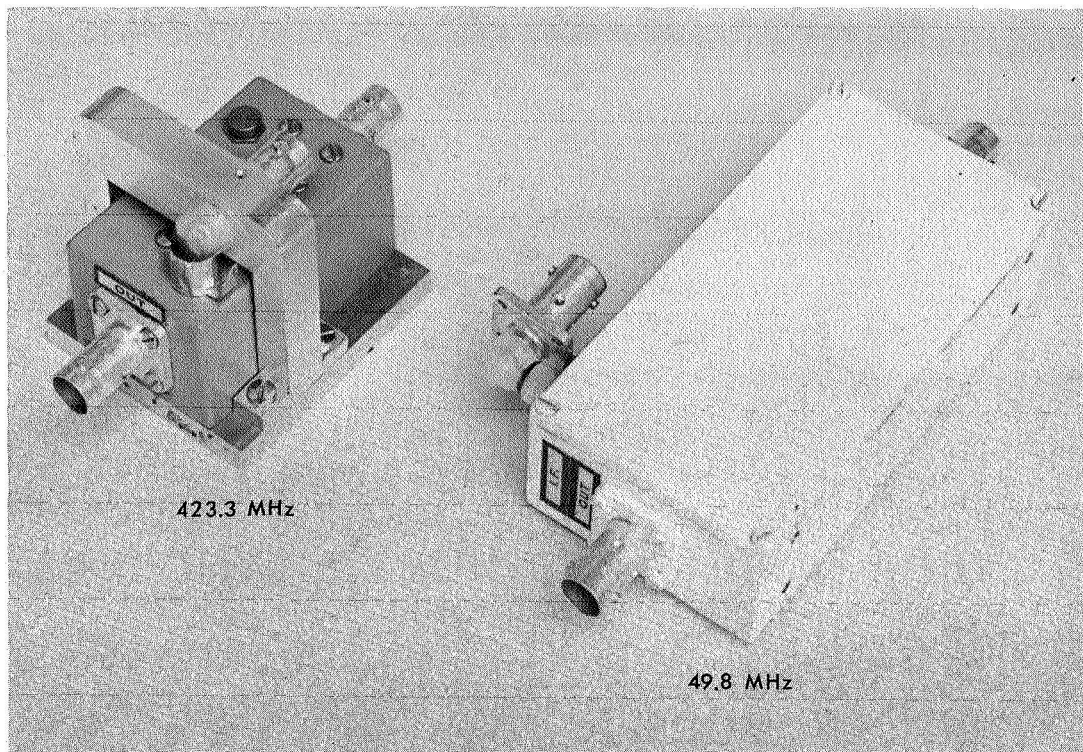


Fig. 7. Low-noise preamplifiers

placing this unit on the spacecraft, close to the UHF antenna during tests, an overall noise figure of approximately 2.4 dB was obtained. The bandwidths of the UHF preamplifier and mixer were wide enough to permit investigating both the 423.3 MHz receiver frequency and the 473.1-MHz image frequency without an additional preamplifier and mixer; however, it was necessary to use two local oscillators. The local oscillator frequencies were selected to translate the 423.3- and 473.1-MHz frequencies to 27 MHz for reception by the R390A/URR high-frequency receiver. Consideration was given in the design for adequate filtering on all power leads, reduction of spurious outputs, and IF selection for image rejection.

2. VHF noise detection instrumentation. For the VHF frequency at 49.8 MHz, a commercial preamplifier/mixer/IF amplifier/local oscillator combination was obtained. The unit had a gain of 70 dB, image rejection greater than 50 dB and a noise figure of 1 dB. The IF output was specified at a frequency of 30.0 MHz so that the output signals could be examined directly with the R390A/URR receiver. The VHF noise detection instrumentation block diagram is shown in Fig. 10. Excellent sensitivity was obtained by placing the preamplifier near

the spacecraft VHF antenna and monitoring the IF output at a remote location. Double-shielded coaxial cables were used for the IF signal and the dc power line.

3. Portable VHF/UHF low-noise receiver. A battery-operated portable noise-detecting receiver loaned by the Stanford University DFR project manager was used extensively in the noise investigation. The receiver was tunable over a 4-MHz range to allow searching for discrete frequencies. The noise figure of the receiver was 3 dB at 49.8 MHz, and 6 dB at 423.3 MHz. Although the receiver did not permit accurate frequency or amplitude noise measurements, the low-noise figure of the unit at 49.8 and 423.3 MHz, and its portability (it was approximately $2 \times 10 \times 12$ in.), allowed it to be used in a variety of applications. The receiver was very useful in the spacecraft test area prior to each test to search out and identify noise sources external to the spacecraft, so that the background ambient noise temperature could be substantially reduced by turning off equipment the receiver identified as a noise source. The unit also proved to be extremely valuable in providing qualitative information during laboratory tests of subsystem noise levels.

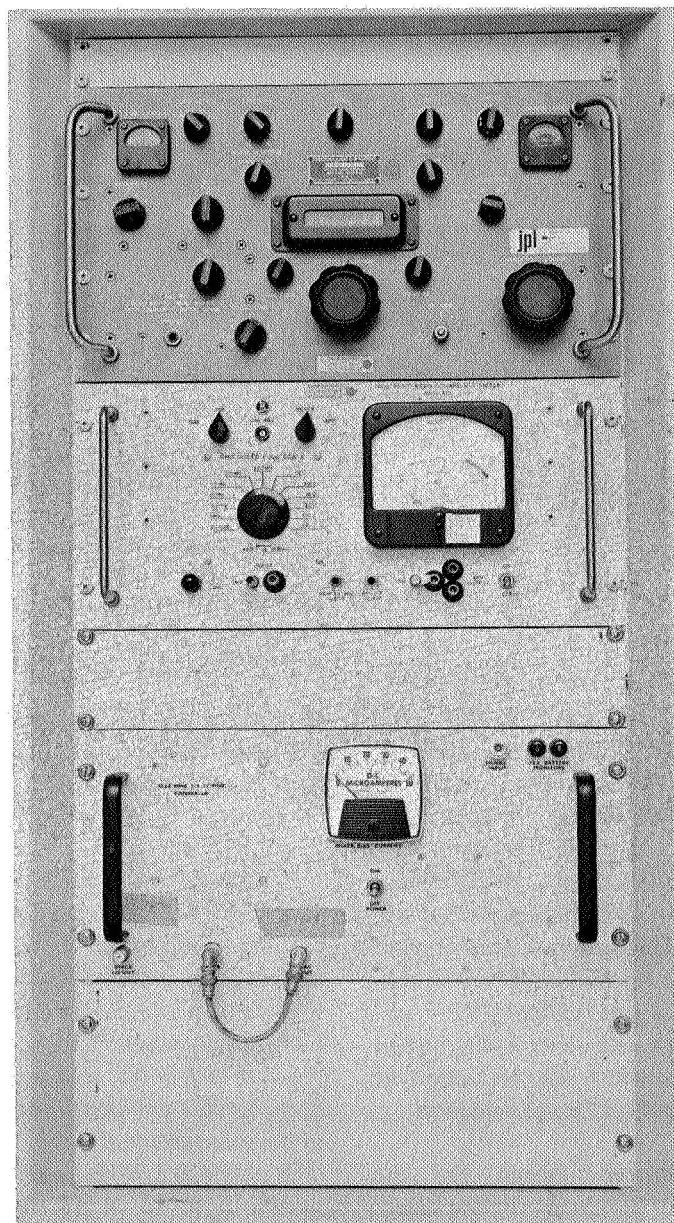


Fig. 8. Noise detection instrumentation console

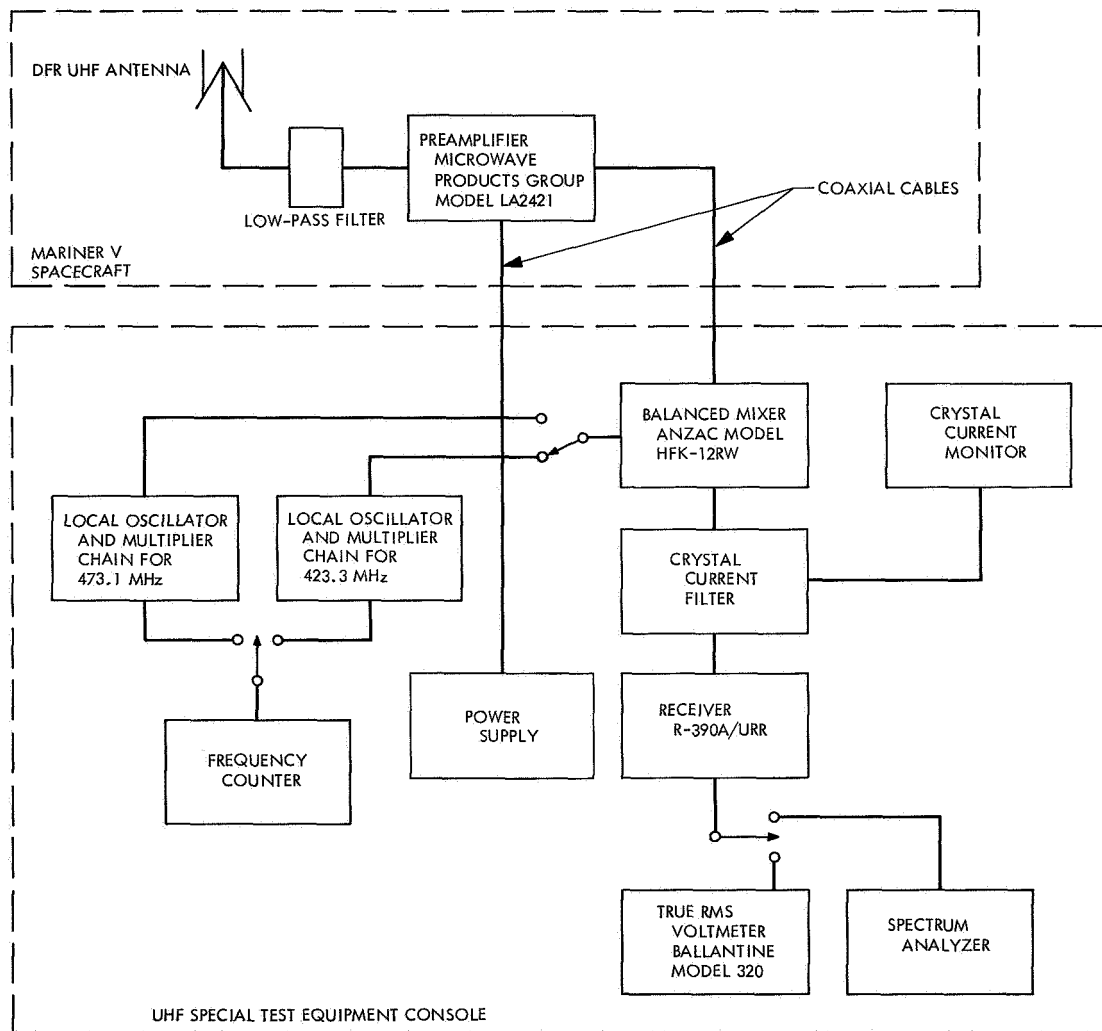


Fig. 9. UHF noise detection instrumentation block diagram

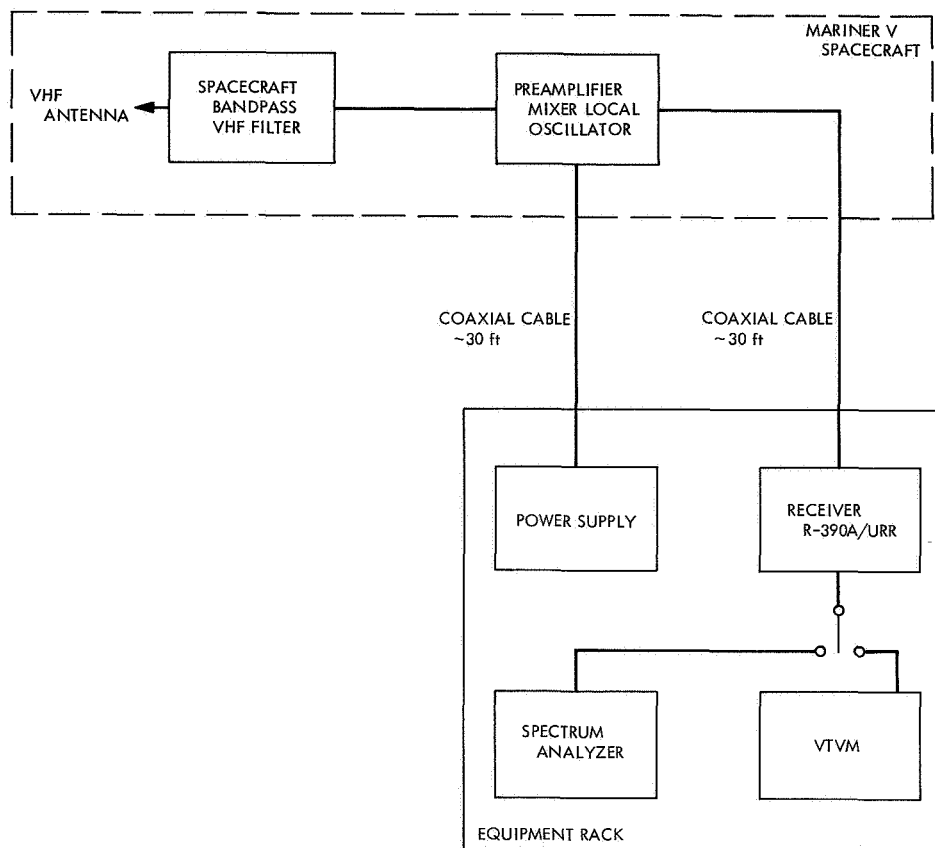


Fig. 10. VHF noise detection instrumentation block diagram

D. Noise Level Calculations

It was necessary to determine how much the DFR would be degraded by noise generated by the spacecraft in a space environment. In space, cosmic noise is present and forms part of the receiver(s) background noise. During tests performed on earth, receiver noise was contributed from sources that are not present in space; e.g., fluorescent lights, electric motors, power regulators, etc. It was necessary, therefore, to determine the noise contributed by just the spacecraft (in various operating modes) and then calculate the level of degradation based on estimated values of cosmic noise.

Assuming the background noise levels to be flat, over a given frequency range, the magnitude of spacecraft noise can be determined by forming a ratio of unknown-

to-known noise levels. With the test receiver connected to the spacecraft DFR antenna terminals, the magnitude of the unknown noise level could be measured. If the antenna was then replaced by a standard noise source, a second reading could be obtained as a reference level. In practice, it was convenient to use 50-Ω input terminations at room temperature (approximately 290°K), or at the temperature of liquid nitrogen (approximately 77.4°K) to establish a reference level. The lower temperature was provided by submerging a standard impedance termination in liquid nitrogen. When the noise level was low, submerging the termination in liquid nitrogen was preferred because it yielded greater test receiver output changes. Because the test receiver readings were directly proportional to the input power levels over the frequency ranges of interest, a noise power ratio could then be used to calculate the unknown noise level.

$$\left\{ \begin{array}{l} \text{Noise} \\ \text{Power} \\ \text{Ratio} \end{array} \right\} = \frac{\text{Test Receiver Internal Noise} + \text{Unknown Noise Level}}{\text{Test Receiver Internal Noise} + \text{Reference Noise Level}} \quad (2)$$

The test receiver internal noise was a parameter determined by laboratory calibrations.

It is convenient to express the noise power available at the terminals of a receiving antenna or from a resistive load in terms of noise temperature, a concept based on Planck's radiation law for thermodynamic black bodies and Nyquist's theorem for the noise power generated in dissipative electric circuit elements. The relation between temperature and noise power is shown in Eq. (3).

$$P_k = k T B \text{ watts} \quad (3)$$

where

k = Boltzmann's constant (1.38×10^{-23} joules/°K)

B = the receiver bandwidth in Hz

T = the effective temperature of the noise source in °K

Using Eq. (3), Eq. (2) can be written as follows:

$$\left\{ \begin{array}{l} \text{Noise} \\ \text{Power} \\ \text{Ratio} \end{array} \right\} = \frac{k T_e B + k T_A B}{k T_e B + k T_0 B} = \frac{T_e + T_A}{T_e + T_0} \quad (4)$$

where

T_e = the test receiver effective noise temperature in °K

T_0 = the reference noise source temperature in °K

T_A = the unknown noise temperature in °K

Expressing the noise power ratio as δ , and solving Eq. (4) for T_A :

$$T_A = \delta(T_e + T_0) - T_e \quad (5)$$

The unknown noise temperature, T_A , was either the test area background noise or the combined spacecraft and test area background noise level, depending on the test conditions. With spacecraft power off, a noise temperature of T_{A1} was obtained. With spacecraft power on, a second value, T_{A2} , was obtained. The increase in noise temperature from T_{A1} to T_{A2} was caused by spacecraft noise. Therefore,

$$T_{sc} = T_{A2} - T_{A1} \quad (6)$$

where T_{sc} was the effective spacecraft noise temperature.

Because DFR performance was directly related to the background noise level in which it operated, DFR degradation levels measured in spacecraft tests were not the same as would be seen in space, unless the testing background noise temperature was the same as the cosmic noise temperature. This was because spacecraft noise could be masked by high levels of cosmic noise; whereas spacecraft noise could become a predominant factor if the cosmic noise level was of the same order of magnitude as spacecraft noise. The amount of degradation to the DFR from spacecraft noise for a given value of cosmic noise can be calculated using Eq. (7)

$$\text{Degradation} = 10 \log \left(\frac{T_r + T_c + T_{sc}}{T_r + T_c} \right) \quad (7)$$

where

T_r = the DFR noise temperature

T_c = the cosmic noise temperature

T_{sc} = the effective spacecraft noise temperature

IV. Evaluation of Mariner V UHF/VHF Noise Environment

A. DFR/S-Band Transponder Test

The first compatibility test was a subsystem test performed in the laboratory using an engineering model S-band transponder and a prototype DFR from the *Pioneer* program. Although the subsystems were not of the *Mariner V* design, they were the best representation of *Mariner V* equipment available at the time. Early testing with any DFR and an S-band transponder was considered valuable for gaining insight into the innate characteristics of these two extremely sensitive RF systems. Since only eight months would separate delivery of the first *Mariner V* DFR and the launch date, it was essential to have an early understanding of the DFR if problems were to be solved expeditiously. Although the frequencies of the engineering model transponder differed by more than 2 MHz from the flight transponders, subsequent testing showed that the interactions discovered during this test also existed with the flight transponders. The results of this early testing permitted procurement of the hardware necessary to eliminate the interference between the RF subsystems and to plan and perform special tests prior to the formal spacecraft acceptance test.

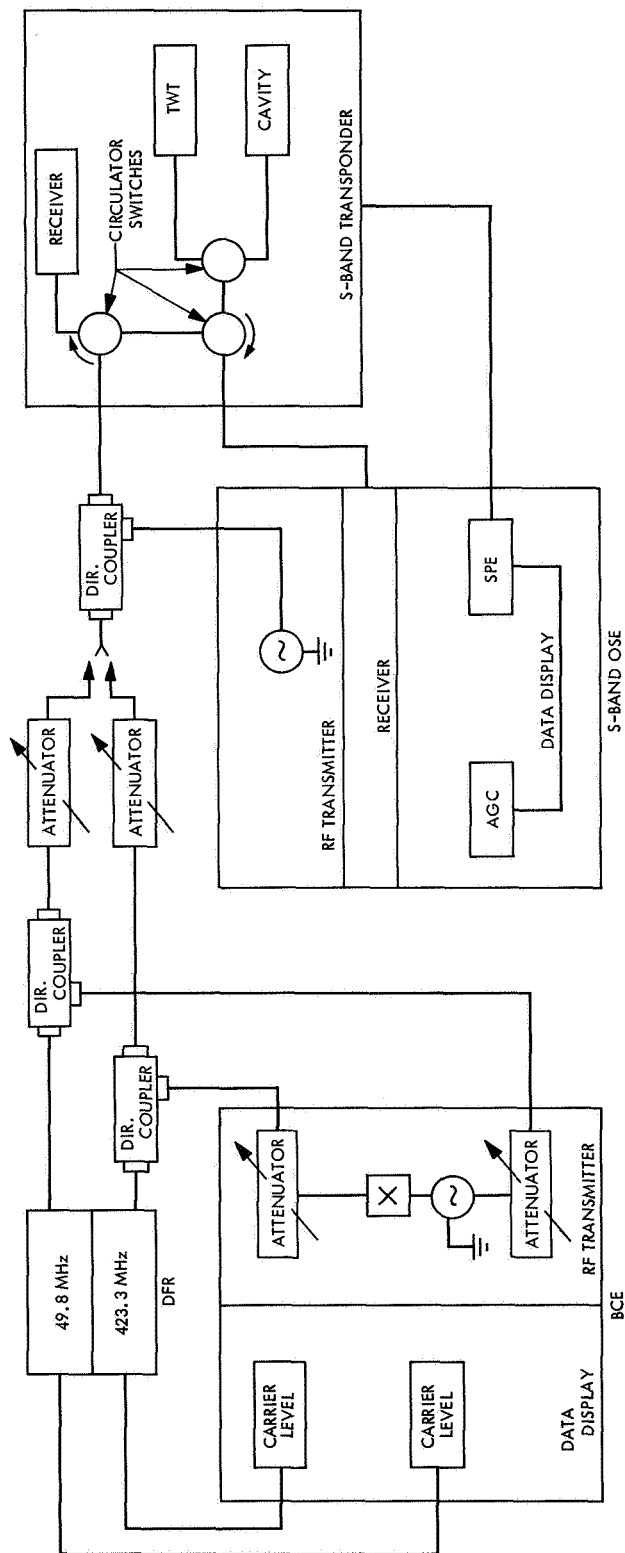


Fig. 11. DFR/S-band transponder test configuration

The S-band/DFR subsystem compatibility test was performed with the subsystems placed next to each other on a conducting surface in a shielded enclosure. Figure 11 shows the test configuration that was selected to provide a worst-case condition for interaction between the subsystems. The antenna connections of both subsystems were connected by attenuators and directional couplers. The purpose of this test configuration was to enable both subsystems to be exercised and, at the same time, to provide a path for coupling signals at the antennas of each subsystem into the receiver under test. With the subsystems in the test configuration, each receiver was exercised and at the same time observed for any signs of interference. When interference was observed, the coupling between the subsystems was decreased by increasing the attenuation. In this manner, a measure of the isolation required between the two subsystems to prevent interference was obtained. The results obtained from these tests are described in the following sections.

1. Interaction of local oscillator harmonics. The Pioneer prototype/S-band compatibility (PP/S-B) tests indicated there was a -3.5 -dB change in the sensitivity of the 423.3-MHz channel of the DFR when the S-band receiver and the DFR receiver were connected. An attenuation of 3 dB eliminated the apparent interference.

It should be pointed out that the 3.5-dB reduction in receiver performance could have resulted from an impedance mismatch between the receiver and transmitter in the test setup. Regardless of the cause, more than 3 dB of isolation existed between the DFR and S-band antennas; therefore, interference of this type would not exist with the subsystems operating on the spacecraft.

2. Intermodulation interference. A computer program was used to determine whether linear combinations of pairs of local oscillator frequencies and other frequencies fell within the RF or IF passbands of the receivers. Two possible intermodulation products were discovered:

- (1) S-band receiver frequency = 2115.699800 MHz
- (2) DFR receiver frequency = 423.300000 MHz

Therefore

$$2115.699800 \text{ MHz} - 4 \times 423.300000 \text{ MHz} \\ = 422.499800 \text{ MHz}$$

$$6 \times 423.300000 \text{ MHz} - 2115.699800 \text{ MHz} \\ = 424.100200 \text{ MHz}$$

While connected to the S-band receiver, the DFR was caused to drift ± 7.5 kHz about 423.3 MHz in search of an output of the S-band receiver upon which to lock; no interfering signals were found.

3. Interaction between S-band transmitter outputs and the DFR. The PP/S-B tests indicated that both channels of the DFR were degraded approximately 27 dB when a 0 dBmW output signal from the TWT amplifier at 2297.5 MHz was coupled into the DFR. It was determined that 60 dB of isolation was required to eliminate the interference.

4. Interaction between DFR outputs and the S-band receiver. The PP/S-B tests indicated that the 50-MHz channel of the DFR could reduce the S-band receiver sensitivity. With the 50-MHz channel of the DFR connected through circulator switch CS-2, a slight increase in S-band static phase error and a 1.3-dB decrease in signal strength was observed. An attenuation of 20 dB was required to eliminate the interference.

When the 423.3-MHz channel of the DFR was connected to the S-band receiver operating at a signal level of -130 dBmW with the ranging receiver and the TWT amplifier on, an S-band signal was generated that would take control of the S-band phase-lock loop. An attenuation of 13 dB between receiver inputs was required to eliminate this interference. No jamming signal was generated by the 423.3-MHz channel of the DFR and the TWT amplifier when the ranging receiver was off.

Based on the results of this test, the following recommendations were made:

- (1) That RF filters, preferably bandpass, be installed at the input to each DFR channel to prevent noise in the 2297.5-MHz frequency band from degrading the DFR sensitivity. Such a filter would attenuate any noise outside the filter passband, thereby preventing noise at other frequencies, including the image frequency, from interfering with the DFR. A bidirectional filter in the 423.3-MHz channel would also isolate the spurious signals within the DFR from the S-band receiver.
- (2) That a filter at the output of the S-band transmitters be added to prevent radiation of noise at 49.8 and 423.3 MHz, thus ensuring that the sensitivity of the DFR channels would not be degraded.

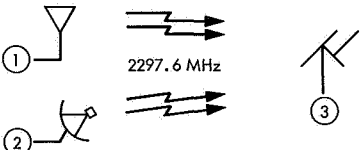
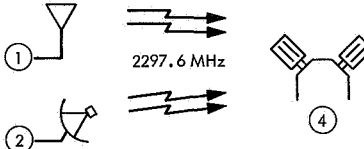
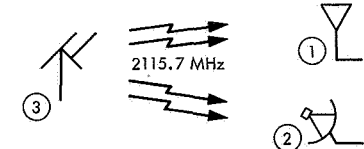
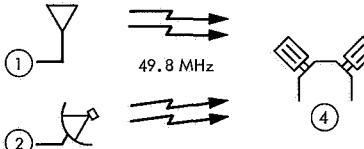
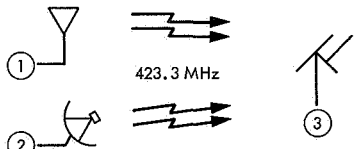
			ISOLATION	
			MEASURED, dB	REQUIRED, dB
	①	2297.6 MHz	① to ③ 68.0	60 (ESTIMATE)
	②		② to ③ 62.5	60 (ESTIMATE)
	①	2297.6 MHz	① to ④ 68.0	60
	②		② to ④ 57.5	60
	③	2115.7 MHz	③ to ① 69.2	13
	②		③ to ② 54.5	13
	①	49.8 MHz	① to ④ 78.0	40 (ESTIMATE)
	②		② to ④ 73.0	40 (ESTIMATE)
	①	423.3 MHz	① to ③ 93.0	40 (ESTIMATE)
	②		② to ③ 79.0	40 (ESTIMATE)
^a ① = S-BAND LOW-GAIN OMNIDIRECTIONAL ANTENNA ② = S-BAND HIGH-GAIN DIRECTIONAL ANTENNA			③ = 428.3-MHz ANTENNA ④ = 49.8-MHz ANTENNA	

Fig. 12. DFR/S-band antenna coupling measurements

- (3) That the following measurements be made to determine the coupling coefficients between the antennas of the spacecraft RF subsystems:
- The level of a 2297.5-MHz signal transmitted from the S-band antennas and received by the DFR antennas.
 - The coupling of a 49.8- and a 423.3-MHz signal transmitted from the S-band antennas and received by the respective DFR antenna.
 - The level of a 2115.7-MHz signal received by the S-band antennas when transmitted from the 423.3-MHz DFR antenna.

The results of the recommended antenna coupling measurements were a determining factor in the procurement of filters. Since the DFR did not possess preselector filters, the installation of bandpass filters ensured that each channel was relatively insensitive to frequencies outside its intended bandpass. The recommended DFR filters would not eliminate noise at the operating frequencies; such noise would have to be reduced at its source or the coupling coefficient decreased. The recommendation for a noise suppression filter at the TWT output was intended to decrease the coupling coefficient; however, its procurement depended on the antenna coupling measurements. If the noise coupled between the

S-band transmitter and the DFR through the antennas was adequately attenuated, a filter at the output of the TWT would not be required.

Antenna RF coupling tests were subsequently performed. The test results are shown in Fig. 12. Based on the results, it was determined that a sufficient decoupling margin existed for noise from the S-band RF power amplifiers at 49.8 and 423.3 MHz, but that the decoupling between the S-band and DFR antennas at 2297.5 MHz was marginal. To provide sufficient isolation between the DFR and the 2297.5-MHz signal from the S-band power amplifiers, it was necessary to add filters at the inputs to the DFR (Fig. 13). Ideally, from the standpoint of noise isolation, bandpass filters would be used. However, in the case of the 423.3-MHz channel, a low-pass filter with an insertion loss of 0.05 dB was used instead of a bandpass filter with an insertion loss of 0.5 dB. Tests showed that a low-pass filter provided the necessary isolation for the 423.3-MHz channel without significantly reducing the already marginal signal level at the 423.3-MHz receiver frequency. Concern about the signal level of the 423.3-MHz channel of the DFR was a result of the limited ground transmitter output power at this frequency.

B. System Level Tests

Figure 14 shows the spacecraft configuration for the early system level tests. All spacecraft subsystems were not available for these early tests since subsystem de-

liveries to the spacecraft assembly facility occurred over a six-month period. To postpone testing until a complete spacecraft was available would have delayed EMI system testing until four months prior to launch. Although conclusive results could not be obtained using a partially assembled spacecraft, these early tests established the need, techniques, and direction for further testing. From these initial tests, three significant facts were learned:

- (1) The 50-MHz noise, generated by spacecraft subsystems, was present at the VHF antenna at a level sufficient to seriously degrade the VHF channel of the DFR. The sources of this 50-MHz noise were the power subsystem booster regulators, battery charger, and the radio subsystem RF amplifier power supplies. Calculated values of DFR degradation from these noise sources ranged from 3 to 11 dB depending on what combination of noise sources were operating.
- (2) No significant amount of noise existed in the 423.3-MHz frequency band of the UHF channel of the DFR.
- (3) Operating without a shielded test facility the background noise level during the daylight hours was too high and too unstable to permit noise tests to be performed. To obtain a noise background low and stable enough required testing between the hours of 10 pm and 6 am PST.

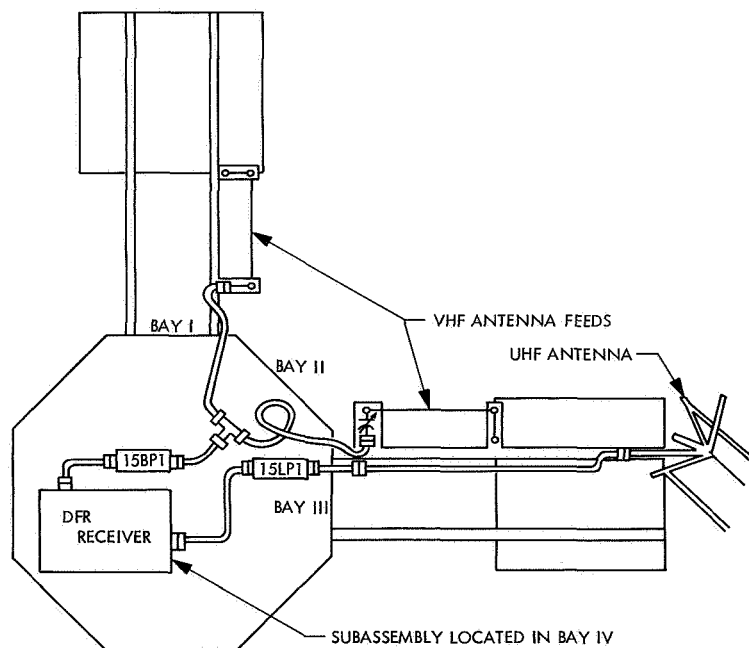


Fig. 13. DFR antennas and filters

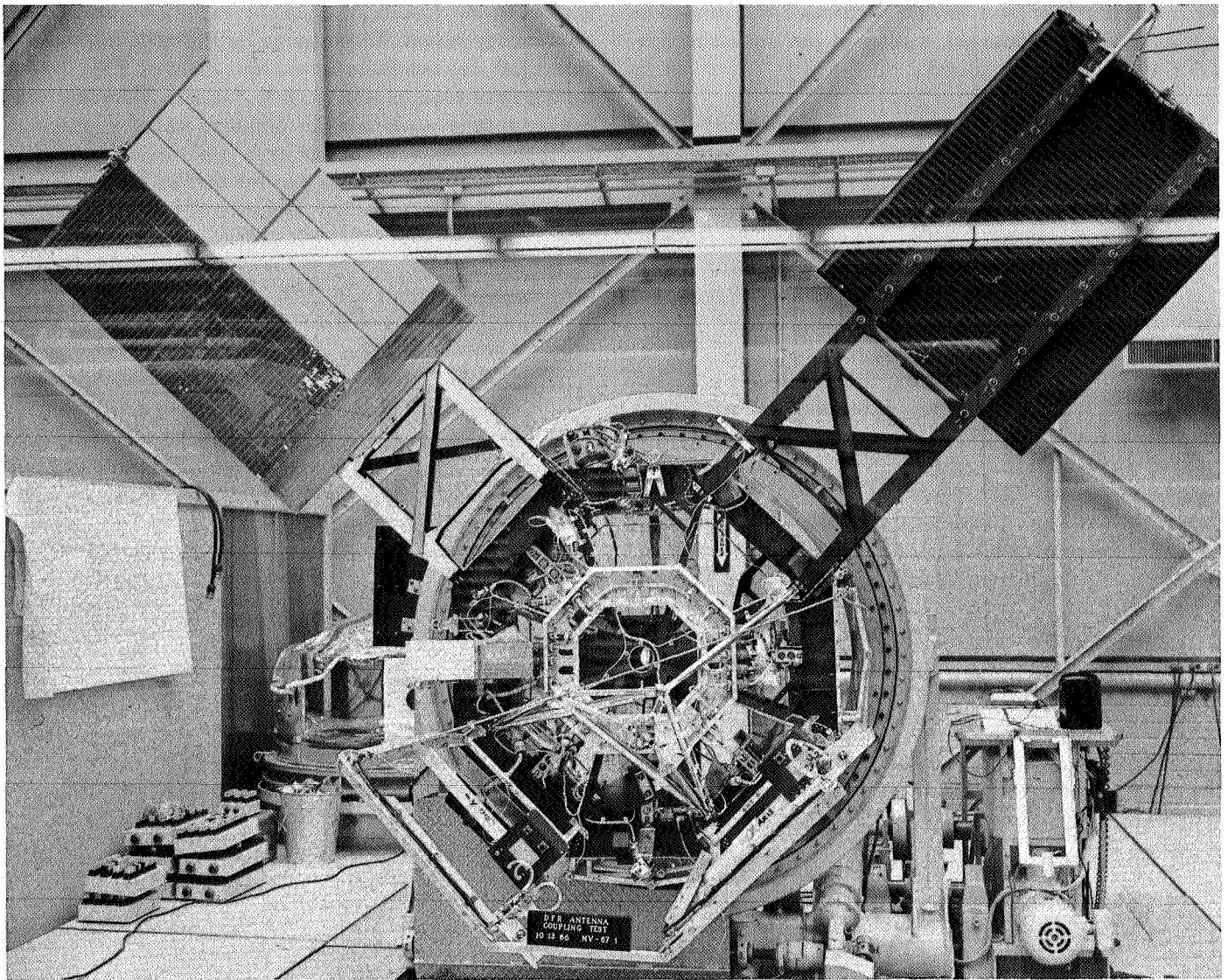


Fig. 14. Spacecraft test configuration

Another interesting result from these spacecraft tests was the discovery of a 4-dB difference in the near field gain of two different sets of 50-MHz antenna feeds. The spacecraft solar panels served as the antenna for the VHF channel of the DFR. Feed wires were connected to adjacent solar panel spars to couple the RF energy from the panels to the receiver. The original design of the 50-MHz antenna feeds called for stainless steel wire. However, antenna tests indicated that the resistive losses of the stainless steel seriously reduced the antenna's efficiency. To decrease the resistance of the feeds, the feed wires were silver-plated and then covered with a coating of gold. With the gold feeds, the 50-MHz antenna was able to meet its gain requirements of 2.0 ± 2.5 dB. An increase

in the spacecraft noise level at the 50-MHz antenna was expected using the gold-plated feeds. However, EMI tests showed that the near field gain of the stainless steel feeds was 4 dB higher than the gold-plated feeds. This rather fortunate situation provided a much-needed effective increase in test receiver sensitivity.

Following the identification of noise sources by the spacecraft tests, subsystem investigations were initiated to develop means for suppressing the generation of RF noise or its coupling into the DFR.

1. Power subsystem noise investigation — booster regulators. The function of the power subsystem booster

regulators is to take a variable dc voltage input and generate a regulated 52-V dc output. The solar panels and spacecraft battery connected in parallel through isolation diodes is the input to the booster regulator. Various factors such as sun-spacecraft distance, battery charge level, solar panel temperature, and solar cell damage from radiation and micrometeorites can cause the booster regulator input voltage to change. The booster regulator was designed to operate with input voltage variations between 25 and 50 V. The power subsystem included two booster regulators: (1) a maneuver booster regulator to power a 2.4-kHz single-phase inverter and a 400-Hz three-phase inverter for attitude control and gyro power during spacecraft maneuvers, and (2) a main booster regulator that drove a 2.4-KHz single-phase inverter that supplied power to all spacecraft and scientific instruments throughout the mission.

A simplified diagram of a booster regulator is shown in Fig. 15(a). The booster regulator maintained voltage

regulation by comparing its output voltage to a reference in the voltage sensing circuit. The sensing circuit in turn controlled the duty cycle of the chopper so that the output of the rectifier when added to the input voltage produced 52 V at the booster regulator output.

Tests performed on the spacecraft identified the power subsystem booster regulators as generators of 50-MHz noise at a level that coupled into the VHF receiver causing a threshold degradation of 5 dB. The source of noise generation was discovered to be large current spikes produced each time diodes CR-1, 2, and 3 were reverse-biased. When a diode is switched from forward to reverse bias, the storage of minority carriers in the body of the device can cause large transient reverse currents. The existence of this type of effect is expected because of the diode junction capacitance. However, the magnitude of reverse current that develops when a diode is reverse-biased is much larger than would result from junction capacitance. The large reverse current at the

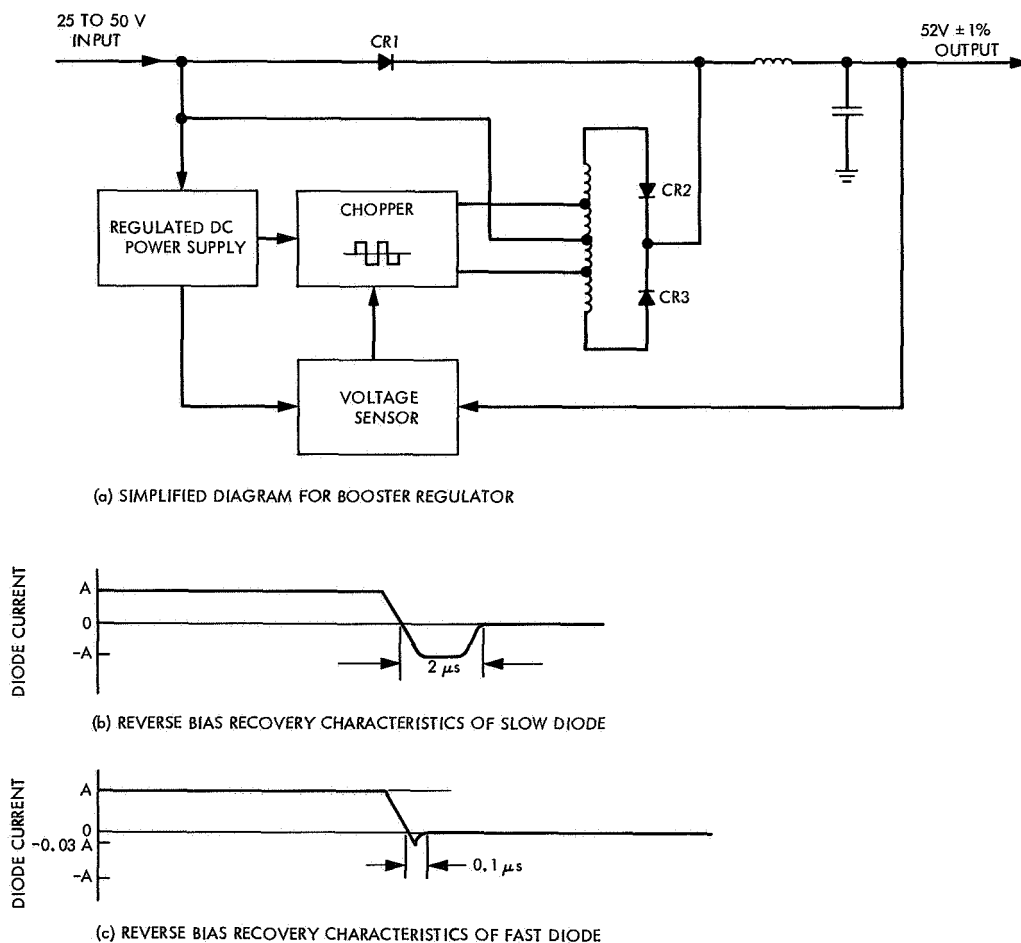


Fig. 15. Power subsystem noise sources

instant of switching results from the high density of minority carriers near the junction that have to be depleted before the diode reaches its steady-state reverse current. For the slow-recovery diodes used in the booster regulator, Fig. 15(b) shows that at the first instant after a reverse bias is applied, a reverse current equal in magnitude to the forward current exists. These reverse current spikes occur approximately every 200 μ s. The amplitude of the frequency components of the spikes relates directly to the total energy contained in the spike. The amplitude of the components in the 50-MHz range of the spike produced by the slow-recovery diodes was sufficient to couple into the DFR at a magnitude that degraded the VHF receiver by 5 dB. It was expected that any 50-MHz noise generated in the booster regulators would interfere with the DFR since the booster regulators were connected to the solar panels, two of which served as the 50-MHz antenna.

To eliminate the noise problem, diodes CR-1, 2, and 3, shown in Fig. 15(a) were replaced with faster diodes. A diode with faster recovery reduced the reverse bias recovery time, as shown in Fig. 15(c), by reducing the lifetime of the carriers, thereby reducing the total energy contained in the noise spike. Incorporating faster recovery diodes in the booster regulator reduced the 50-MHz noise level such that the spacecraft booster regulators contributed less than 1 dB of degradation to the DFR.

2. Battery charger. Spacecraft tests also showed the battery charger to be a 50-MHz noise source. Because the battery charger used the same type diodes in the same fashion as the booster regulator, these diodes were the suspected noise generators in the battery charger. Noise generated by the battery charger was not as detrimental as booster regulator noise since the spacecraft flight sequence could be controlled so that the battery charger would not be operating during those critical periods of DFR operation. This, and cost and time constraints, were reasons enough not to change the diodes in the battery charger.

C. S-Band Transmitter Power Supply Noise Investigation

Preliminary noise measurements made during the initial spacecraft noise investigations with the 50-MHz test instrumentation indicated that noise originating in the engineering model S-band transmitter power supplies would degrade the VHF receiver sensitivity by as much as 11 dB. A noise reduction investigation was initiated and verified that an envelope of noise containing har-

monics of the power supply switching frequency (11 kHz) existed at 50 MHz. Noise reduction methods such as shielding, ferrite bead filters, and bypass capacitors were evaluated in an effort to reduce the 50-MHz noise level from the power supplies.

Subsequent tests using a DFR and S-band transmitter power supplies showed that no more than 1 dB of degradation occurred to the DFR from either a modified or unmodified power supply. Subsequent testing with a power supply and the DFR removed from the spacecraft and operating in an anechoic chamber showed DFR degradation levels of as much as 28 dB. However, no more than 1 dB of degradation was ever observed by the DFR as a result of noise generated by the power supplies when the subsystems were operating on the spacecraft.

The inconsistency in the noise level measurements was not completely understood. Other tests showed a close correlation between test receiver data and DFR degradation levels. This discrepancy could be explained by a varying coupling coefficient between the DFR antenna and the noise sources. The fact that the spacecraft was not completely assembled during the early tests supports this hypothesis. Because of the magnitude of effort required to make noise measurements on the spacecraft and lack of time, further investigation into this discrepancy was not possible.

D. DAS Noise Investigation

While the first production model of the data automation subsystem (DAS) was being interfaced on the *Mariner Venus 67* spacecraft, a cursory examination of the noise level of the science subsystem was performed. The science instruments on the spacecraft at this time were the magnetometer, the trapped radiation detector, and the ultraviolet photometer. The DFR was not on the spacecraft during this testing. This cursory examination was made with the portable 49.8- and 423.3-MHz test receiver and indicated that the 49.8-MHz noise emanating from the DAS was greater than that of any other subsystem investigated. Spacecraft tests using the DFR indicated that the threshold of the 50-MHz channel was degraded by more than 16 dB as a result of RF noise radiated by the DAS. Further investigations revealed that the major source of interference from the DAS was the 112th harmonic of the DAS master oscillator (Fig. 16). The DAS master oscillator frequency was 444.444 kHz, the 112th harmonic of this frequency was 49.777728 kHz. The 112th harmonic was, therefore, 228 Hz inside the 45-kHz 3-dB IF bandwidth of the

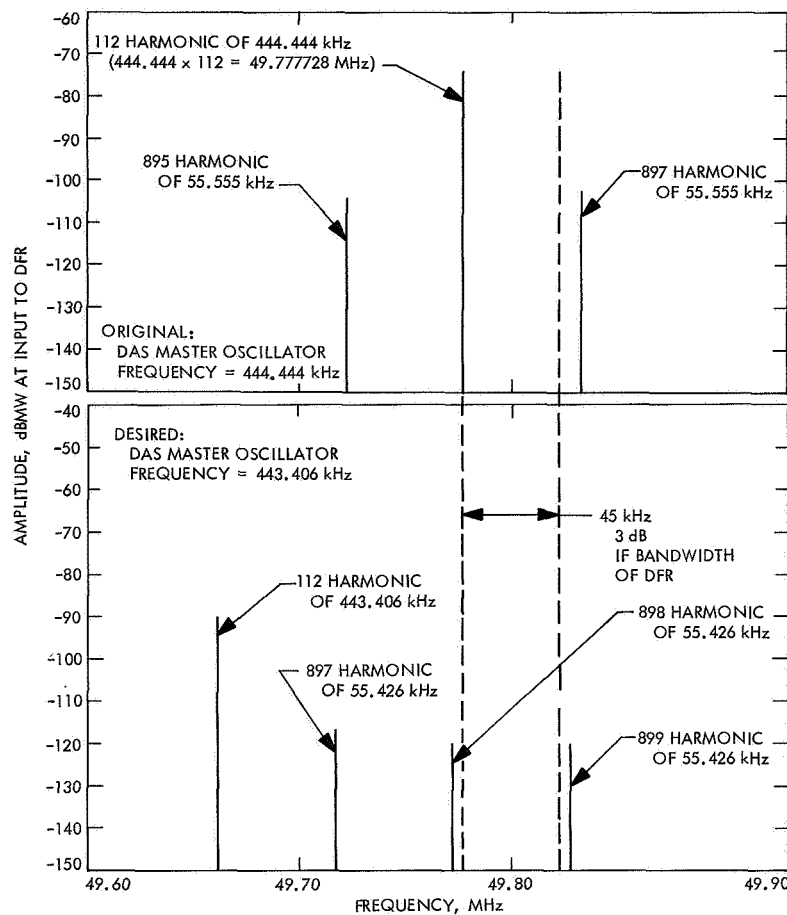


Fig. 16. DAS master oscillator harmonics

DFR. The presence of this discrete RF signal only 22.272 kHz from the receiver frequency of the 49.8-MHz channel of the DFR was the major source of noise from the DAS. Also, in the DAS, the 444.444-kHz master oscillator frequency was used to generate a 55.555-kHz signal. Therefore, there were eight other discrete signals 55.555 kHz apart between every harmonic of the 444.444-kHz signal. The harmonics of the 55.555-kHz signal, although 40 dB lower in amplitude than the harmonics of the 444.444-kHz signal, also interfered with DFR operations. To reduce the interference from the DAS master oscillator, the obvious solution was to move the 112th harmonic out of the IF passband of the DAS by changing the master oscillator frequency.

Drastic changes could not be made to the DAS master oscillator frequency because DAS logic was based on timing signals generated from the 444.444-kHz oscillator. Small changes in the master oscillator frequency could be tolerated; large changes would seriously affect DAS

operation. Tests showed that reducing the frequency of the master oscillator by 1 kHz eliminated the major portion of DFR interference from the DAS without degrading the operation of the DAS. The selection of a new frequency for the DFR master oscillator was based on three constraints:

- (1) The change in oscillator frequency should be as small as possible. Since the 112th harmonic lay on the lower frequency side of the DFR IF bandwidth, a reduction in oscillator frequency would provide the greatest noise reduction for the smallest change in oscillator frequency.
- (2) The 112th harmonic should be moved from the 3-dB DFR IF amplifier bandwidth by approximately 110 kHz — two 55.555-kHz harmonics.
- (3) The 898th and 899th harmonics of the 55.555-kHz harmonics should be centered about the 49.8-kHz DFR receiver frequency. These constraints re-

sulted in the following equation used to determine the new DAS master oscillator frequency:

$$112x + \frac{2}{8}x + \frac{1}{16}x = 49.8 \text{ MHz}$$

where

x = desired DAS master oscillator frequency

$x = 443.406 \text{ kHz}$

Changing the frequency of the DAS master oscillator to 443.406 kHz placed the two 55.426 kHz harmonics 5.213 kHz away from each side of the 45-kHz 3-dB IF bandwidth of the DFR. The only approach for decreasing the interference from the 55.426-kHz discretes was to contain this noise within the DAS, thereby preventing it from coupling into the VHF antenna. Suppressing the noise from the DAS timing circuitry was accomplished by shielding the intraconnecting cables with aluminized Mylar to reduce radiation of signals from the cabling. Ferrite beads that acted as low-pass filters were installed on each wire of the interconnecting cables to reduce the conduction of noise out of the DAS. The shielding on the DAS harness and a test connector with ferrite beads are shown in Fig. 17. The DFR can also be seen in the top center of this figure.

Further testing with the spacecraft indicated that the corrective actions had eliminated the interference between the DFR and DAS.

E. Spacecraft Noise Level Verification Test

Because the noise investigation tests were performed on a partially assembled spacecraft in a nonflight configuration (Fig. 14), a test with a fully assembled spacecraft in a flight configuration was necessary to adequately verify that the DFR was compatible with the spacecraft electromagnetic environment. A test envisioned as feasible for the acceptance testing was one with the spacecraft suspended by nylon lines from a hoist in the Spacecraft Assembly Facility (SAF) as shown in Fig. 18. The spacecraft was completely assembled and operated in its flight configuration utilizing the S-band air link for telemetry and command transmissions.

The verification test employed both the test instrumentation and the flight DFR. With the test instrumentation, a 45-kHz frequency band was scanned. This enabled a search for interfering signals throughout the passband of the DFR. Also, the lower noise figure of the noise detec-

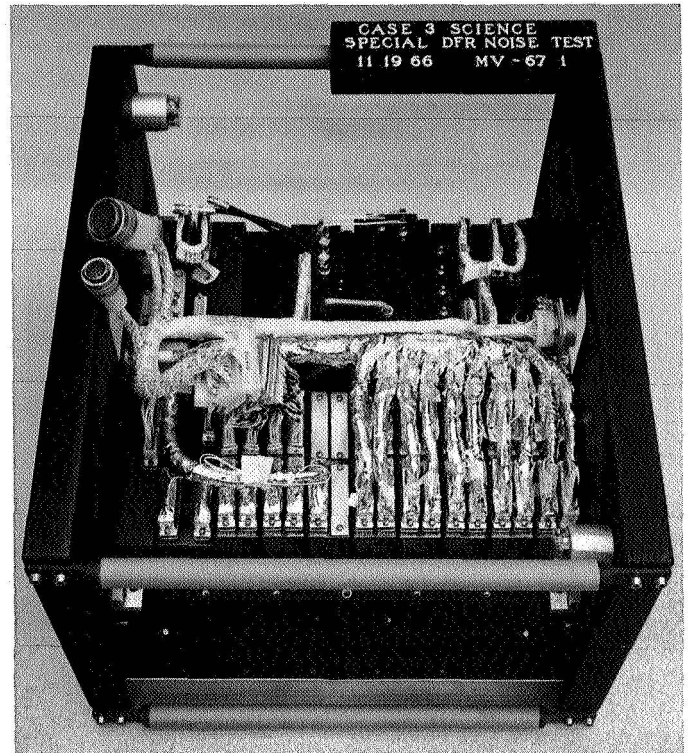


Fig. 17. Spacecraft science case

tion instrumentation permitted measurements at higher background noise levels.

To avoid an effective reduction in the detector sensitivity from losses in the coaxial cables connecting the test instrumentation to the DFR antennas, the RF preamplifiers were installed on the spacecraft and connected to the antennas with short lengths of coaxial cable. The test instrument configuration is shown in Fig. 19.

As discussed in Section III-D, it was necessary to determine the background noise level before spacecraft power was applied. This phase of the test was performed by connecting a known noise source, a 50-Ω termination in this case, to the input of the test instrumentation RF preamplifiers. The received noise power was then recorded. The known noise source was removed and the RF preamplifiers were connected to the spacecraft antennas, again recording the received noise power. The background noise temperatures, T_A , were then determined by calculating the ratio of the noise powers, δ , and using Eq. (5). To aid in calculating effective antenna noise temperatures, a chart based on Eq. (5) was drawn as shown in Fig. 20. Effective antenna noise temperatures can be read directly from the chart by using the noise

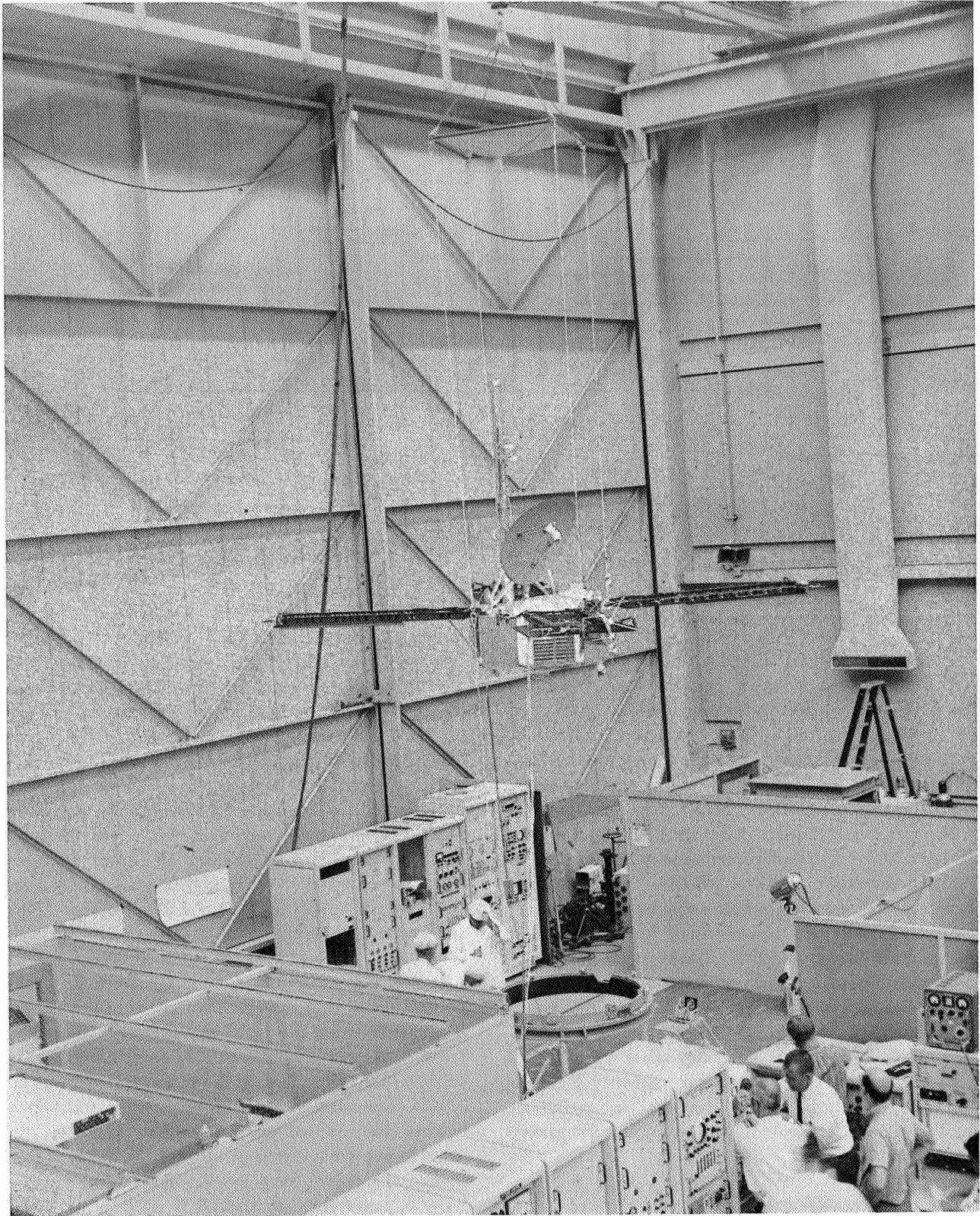


Fig. 18. Suspended spacecraft

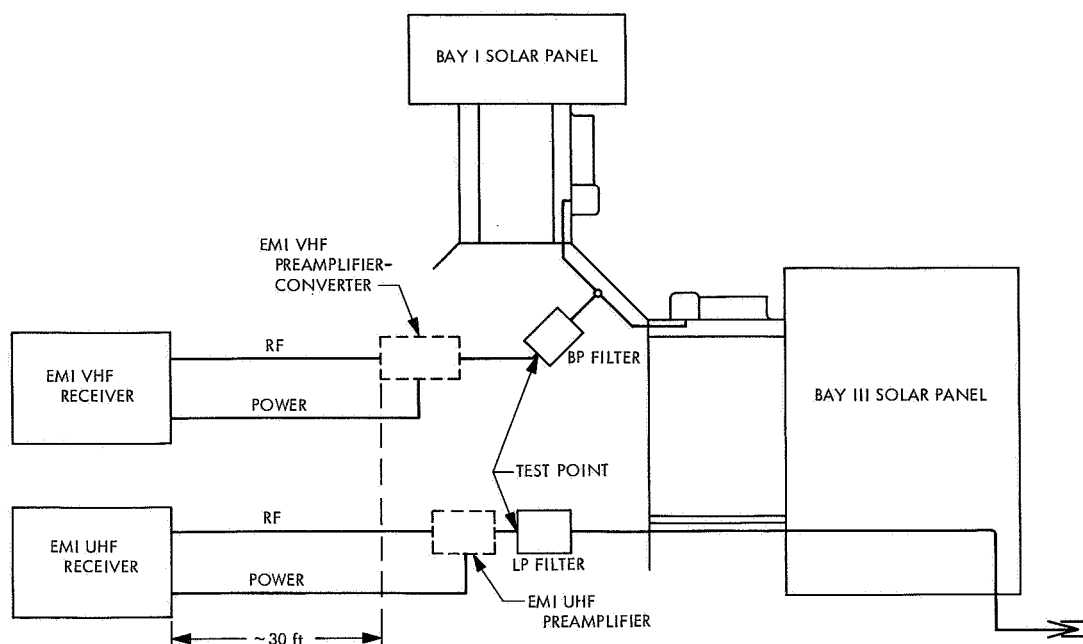


Fig. 19. Spacecraft instrumentation configuration for noise measurements

figure of the test receiver and the difference in received noise power expressed in decibels.

Once the background noise level was determined, spacecraft power was applied. The spacecraft was then exercised through various operations while noise measurements were recorded. Changes in spacecraft noise levels could then be associated with the spacecraft subsystems and their various operating modes. To prevent the possibility of errors caused by a changing ambient noise level, the background effective noise temperature should have been measured prior to every noise measurement. This, however, was not possible because many spacecraft modes required a time-sequenced turn-on. To condition the spacecraft to a required mode could take several minutes during which the background noise level could change. Because an RF screen room large enough to contain *Mariner V* was not available, testing with a changing background noise level represented a significant operational handicap. To compensate for the lack of a screen room, tests had to be performed during periods when the background noise level was relatively stable. The period between 2300 and 0600 PST proved most satisfactory.

To serve as a check for the calculated values of degradation, the DFR was employed in a manner similar to the noise detection instrumentation. Figure 21 shows the test

configuration employed with the DFR. Using the DFR and its bench checkout equipment enabled direct measurements to be made of the DFR amplitude phase-detector output. The output of the amplitude phase-detector was a measure of the received signal-to-noise ratio. Any increase in the background noise level resulted in a decrease in the signal-to-noise ratio. By changing the signal level to maintain a constant signal-to-noise ratio, the change in signal strength was a direct measure of the change in noise level. A direct measure of the noise power seen by the DFR for any given condition could, therefore, be obtained by adjusting the signal output of the bench checkout equipment to establish a signal-to-noise ratio equal to that which existed prior to activating a particular spacecraft operation.

It was also necessary to use the DFR to ensure that no conducted interference resulted from the various connections between the DFR and the other spacecraft subsystems. A check for conducted interference was made with the DFR installed on the spacecraft with its antenna inputs connected to the test transmitter through coaxial cables. The use of coaxial cables prevented radiated interference from entering into the DFR through its antennas. Therefore, any interference to the DFR would have to enter through the DFR cabling. No conducted interference was observed at the DFR while the spacecraft was exercised through all of its operating modes.

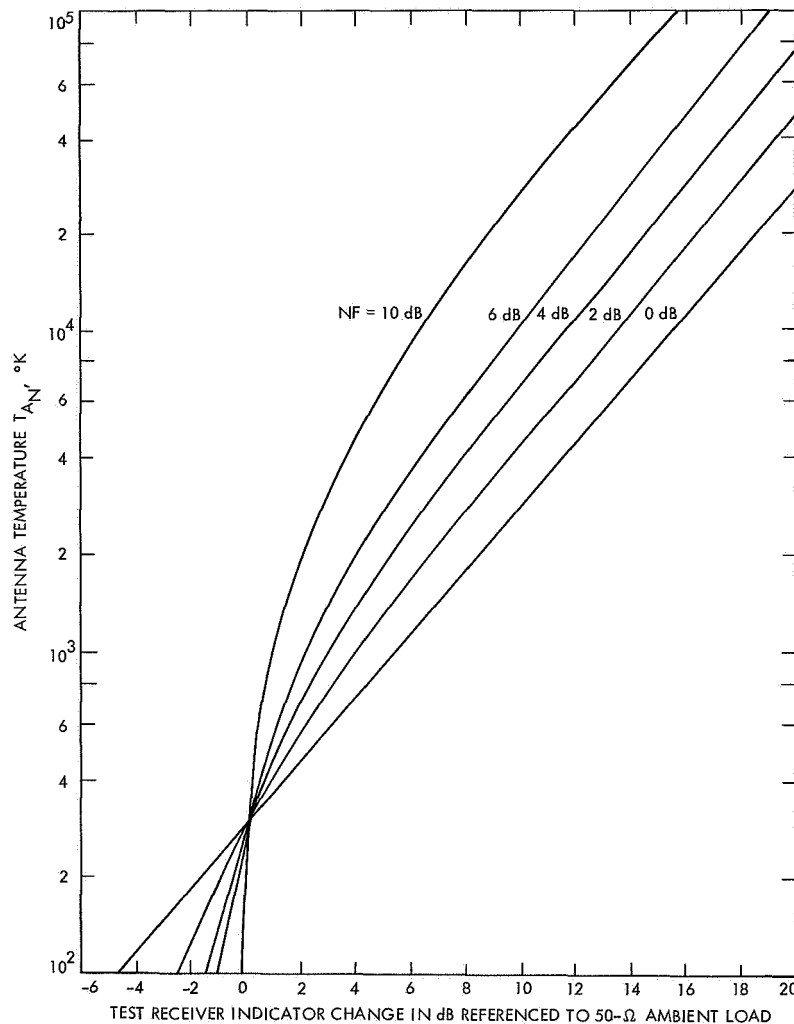


Fig. 20. Noise level changes vs antenna noise temperature

During the verification test, two new 49.8-MHz noise sources were discovered; the ionization pulse applied to the helium-absorption cell of the magnetometer at science power turn-on and attitude-control gas jet actuations. The noise burst at initial ionization of the helium-absorption cell was sufficient to cause more than a 10-dB change in the VHF signal-to-noise ratio. Subsequent pulses used to maintain the ionization level caused less than a 0.5-dB change in the signal-to-noise ratio for a background noise temperature of 5400°K. Since science power was applied at the beginning of the cruise phase and maintained on for the duration of the mission, the noise burst at initial power turn-on of the magnetometer was acceptable. Each attitude control actuation of the spacecraft solenoid-controlled gas valves produced 49.8-MHz noise bursts. Since the noise was of short duration and resulted in approximately 0.5 dB reduction to the

VHF signal-to-noise ratio for a background noise temperature of 5400°K, the noise from gas jet actuations was acceptable.

As part of the test, the VHF test instrumentation was used to verify that the data automation subsystem master oscillator harmonics were indeed removed 27.713 kHz from the VHF center frequency (Fig. 16) and that no other discrete noise sources were present within a 55-kHz band centered at 49.8 MHz.

The verification test showed that the spacecraft noise level had been reduced below the specified 3 dB for the 49.8-MHz channel and 1 dB for the 423.3-MHz channel of the DFR. The test data showed that, for a cosmic noise temperature between 6000 and 8000°K, the 49.8-MHz channel would be degraded less than 1 dB. No

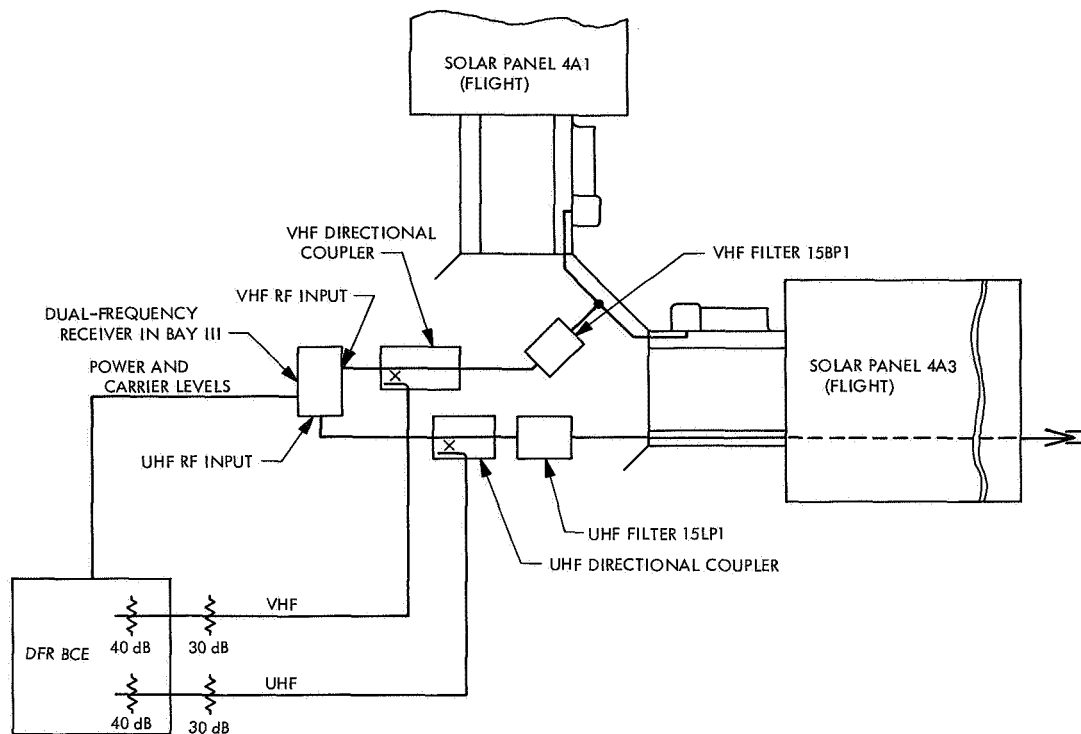


Fig. 21. Dual frequency receiver test configuration

inflight degradation was expected for the 423.3-MHz channel.

F. Summary of Results

Table 1 lists each of the 49.8-MHz noise sources of the *Mariner V* spacecraft. No appreciable spacecraft noise was observed by the 423.3-MHz channel of the DFR. The effect of each 49.8-MHz noise source upon the DFR operating in a 5400°K background noise temperature is given for before and after incorporation of noise reduction modifications. As explained in Section III-D, the effect of spacecraft noise upon DFR flight performance was a function of the cosmic noise level seen by the DFR. The cosmic noise for the 49.8-MHz channel of the DFR was estimated to be between 6000 and 8000°K. For the purpose of calculating DFR degradation for space operation, a 7000°K cosmic noise level was assumed.

It was estimated that to have further decreased the noise level would have required considerably more time and effort than had been expended to obtain the gross changes that were effected. It was felt that to further reduce the residual noise level by any significant amount would have required an entirely new approach to the *Mariner V* design.

V. Conclusions

Sensitive noise receiver systems operating below 420 MHz in close proximity to other electronic devices will suffer receiver performance degradation because electronic devices tend to generate low-frequency broadband noise. This statement is based on the extensive effort required to integrate the 49.8-MHz receiver on-board *Mariner V*. On the other hand, degradation to the 423.3-MHz receiver was virtually nonexistent. It was apparent from the test results that the noise level of the *Mariner* spacecraft and its operational support equipment, much like atmospheric and cosmic noise, increases with decreasing frequency.

No less than total system tests can be used for determining the subsystems which are sources of interference. The necessity for evaluating and verifying equipment operation in its system environment was demonstrated by the results of the tests performed on a partially assembled spacecraft. These early tests indicated that the S-band radio frequency power amplifier power supplies would interfere with the DFR. When the spacecraft was completely assembled, no interference to the DFR was detected from these power supplies. If subsystem testing had been used to identify noise sources, extensive

Table 1. Electromagnetic interference summary

Noise source	Degradation at 49.8 MHz prior to fix	Fix	Degradation at 49.8 MHz after fix	Calculated degradation for space
	Background noise temperature = 5400°K		Background noise temperature = 5400°K	Cosmic noise temperature = 7000°K
S-band TWT amplifier	^a	49.8-MHz bandpass filter, 423.3-MHz low-pass filter	0 dB	0 dB
Science data automation subsystem	16 dB	Change master oscillator frequency by 1.038 kHz. Wrap DAS intraconnecting harness with aluminized Mylar. Install two ferrite beads on each of 200 interconnecting wires	0 dB	0 dB
Booster regulator	5 dB	Change to faster power diodes	0.7 dB	0.6 dB
Battery charger	1 dB	None. Charger can be turned off by ground command if necessary	1.0 dB	0.88 dB
S-band amplifier power supplies	0.5 dB	None	0.5 dB	0.4 dB
Magnetometer ionization pulses	0.5 dB	None. Pulses only occur every 27 hours	0.5 dB	0.4 dB
Gas jet actuations	0.5 dB	None. Pulses are of short duration.	0.5 dB	0.4 dB
^a A 27-dB degradation to both channels of the DFR was observed during the DFR/S-band transponder compatibility test. Sixty decibels of isolation between the DFR and the S-band traveling-wave-tube amplifier was required to completely eliminate the interference. Antenna coupling measurements showed that approximately 57 dB of isolation existed between the VHF and S-band high-gain antennas, while 62 to 68 dB of isolation existed for other coupling paths. To ensure sufficient isolation between the DFR and the S-band transponder, filters were installed at the DFR inputs.				

amounts of time and money would have been spent trying to eliminate a problem that did not significantly affect the total system.

The spacecraft test model available early in the program was an invaluable tool for providing the system environment needed to ensure a valid evaluation of the electromagnetic environment established by each subsystem operating in its system configuration. The test model spacecraft also reduced the time and money costs of problem solving by providing a test vehicle that was not constrained by the rigid requirements placed on flight hardware.

A small, battery-operated receiver with a noise figure equal to that of the DFR, was a valuable asset to the program. Although it was impossible to quantitatively

relate the noise response of this test receiver to DFR performance, the ability to quickly evaluate relative changes in noise levels, after incorporating design changes, significantly reduced the time required to evaluate noise suppression techniques. The portable test receiver was also ideal for pin-pointing the location of noise sources.

Successful EMI testing was accomplished on *Mariner V* using an unshielded test facility. An acceptable test environment was obtained by identifying and eliminating interfering noise sources within the test facility using the portable test receiver and avoiding interfering noise sources external to the test facility by testing between 2200 and 0600 hours. This approach resulted in 49.8 MHz test facility background noise temperatures as low as 1300°K as compared to 20,000°K or higher noise levels during the daylight hours.

Appendix

Example Noise Level Calculation

Assume a noise power increase of 4 dB as measured by the test receiver when the input to the test receiver is changed from a 50- Ω terminator at 290°K to an antenna. With spacecraft power OFF, the noise power at the antenna is background noise. The effective background noise temperature, T_A , can be calculated using Eq. (5) of Section III-D:

$$T_A = \delta(T_e + T_o) - T_e \quad (\text{A-1})$$

Converting the 4-dB increase in received noise power to numeric value gives:

$$\begin{aligned} 4 \text{ dB} &= 10 \log \delta \\ \delta &= 2.5 \end{aligned}$$

Given a receiver noise temperature $T_e = 300^\circ\text{K}$ and a 290°K temperature for the 50- Ω termination, $T_o = 290^\circ\text{K}$, the effective background noise temperature at the antenna is:

$$\begin{aligned} T_A &= 2.5(300 + 290) - 300 \\ T_{A1} &= 1175^\circ\text{K} \end{aligned}$$

With the test receiver connected to the antenna, assume an 8-dB increase from the 50- Ω termination noise level when spacecraft power is applied. Again, using Eq. (A-1), the effective antenna noise temperature is calculated.

$$\begin{aligned} 8 \text{ dB} &= 10 \log \delta \\ \delta &= 6.3 \end{aligned}$$

$$T_A = 6.3(300 + 290) - 300$$

$$T_{A2} = 3417^\circ\text{K}$$

Using Eq. (6) of Section III-D, the effective spacecraft noise temperature, T_{sc} , is:

$$\begin{aligned} T_{sc} &= T_{A2} - T_{A1} \\ &= 3417 - 1175 \\ &= 2242^\circ\text{K} \end{aligned}$$

The level of receiver degradation in a background noise temperature different from the test environment can be calculated using Eq. (7) of Section III-D:

$$\text{Degradation} = 10 \log \frac{T_r + T_{sc} + T_c}{T_r + T_c} \quad (\text{A-2})$$

For the VHF channel of the DFR, $T_r = 300^\circ\text{K}$. Cosmic noise temperature T_c was estimated to range from 6000 to 8000°K. Spacecraft noise temperature, T_{sc} , was calculated to be 2245°K.

The DFR VHF receiver degradation in space with a 7000°K cosmic noise temperature from a spacecraft noise temperature of 2245°K would be

$$\begin{aligned} \text{Degradation} &= 10 \log \frac{300 + 2242 + 7000}{300 + 7000} \\ &= 10 \log 1.3 \\ &= 1.1 \text{ dB} \end{aligned}$$

Bibliography

1. Greiner, R. A., *Semiconductor Devices and Applications*. McGraw-Hill Book Co., Inc., New York, 1961.
2. Schwartz, M., *Information Transmission, Modulation, and Noise*. McGraw-Hill Book Co., Inc., New York, 1959.
3. *Reference Data for Radio Engineers*, Fourth Edition. International Telephone and Telegraph Corporation, New York, 1956.
4. Koehler, R. L., *A Phase-Locked Dual-Channel Spacecraft Receiver for Phase and Group Path Measurements*. Stanford University, Stanford, California, 1965.
5. "Venus: Ionosphere and Atmosphere as Measured by Dual-Frequency Radio Occultation of *Mariner V*," *Science*, Vol. 158, No. 3809, Dec. 29, 1967.
6. Fjeldbo, G., Eshleman, V. R., Garriott, O. K., and Smith, F. L., III, "The Two-Frequency Bistatic Radar-Occultation Method for the Study of Planetary Ionospheres," *J. Geophys. Res.*, Vol. 70, No. 15, Aug. 1, 1965.
7. *Handbook of Microwave Measurements*, Vol. III, Third Edition. Polytechnic Press of the Polytechnic Institute of Brooklyn, New York, 1963.